EUROPEAN ORGANISATION FOR NUCLEAR RESEARCH (CERN)

Measurement of the flavour composition of dijet events in pp collisions at $\sqrt{s} = 7\ \mathrm{TeV}$ with the ATLAS detector

The ATLAS Collaboration

Abstract

This paper describes a measurement of the flavour composition of dijet events produced in pp collisions at $\sqrt{s} = 7\ \mathrm{TeV}$ using the ATLAS detector. The measurement uses the full 2010 data sample, corresponding to an integrated luminosity of 39 pb^{-1}. Six possible combinations of light, charm and bottom jets are identified in the dijet events, where the jet flavour is defined by the presence of bottom, charm or solely light flavour hadrons in the jet. Kinematic variables, based on the properties of displaced decay vertices and optimised for jet flavour identification, are used in a multidimensional template fit to measure the fractions of these dijet flavour states as functions of the leading jet transverse momentum in the range $40\ \mathrm{GeV}$ to $500\ \mathrm{GeV}$ and jet rapidity $|y| < 2.1$. The fit results agree with the predictions of leading- and next-to-leading-order calculations, with the exception of the dijet fraction composed of bottom and light flavour jets, which is underestimated by all models at large transverse jet momenta. The ability to identify jets containing two b-hadrons, originating from e.g. gluon splitting, is demonstrated. The difference between bottom jet production rates in leading and subleading jets is consistent with the next-to-leading-order predictions.

Measurement of the flavour composition of dijet events in pp collisions at $\sqrt{s} = 7$ TeV with the ATLAS detector

The ATLAS Collaboration

1

Abstract This paper describes a measurement of the flavour composition of dijet events produced in pp collisions at $\sqrt{s} = 7$ TeV using the ATLAS detector. The measurement uses the full 2010 data sample, corresponding to an integrated luminosity of 39 pb^{-1}. Six possible combinations of light, charm and bottom jets are identified in the dijet events, where the jet flavour is defined by the presence of bottom, charm or solely light flavour hadrons in the jet. Kinematic variables, based on the properties of displaced decay vertices and optimised for jet flavour identification, are used in a multidimensional template fit to measure the fractions of these dijet flavour states as functions of the leading jet transverse momentum in the range 40 GeV to 500 GeV and jet rapidity $|y| < 2.1$. The fit results agree with the predictions of leading- and next-to-leading-order calculations, with the exception of the dijet fraction composed of bottom and light flavour jets, which is underestimated by all models at large transverse jet momenta. The ability to identify jets containing two b-hadrons, originating from e.g. gluon splitting, is demonstrated. The difference between bottom jet production rates in leading and subleading jets is consistent with the next-to-leading-order predictions.

Keywords heavy flavour jet · b-jet production · dijet event

1 Introduction

A study of the production of jets containing bottom and charm hadrons, which are likely to have originated from bottom or charm quarks, is of strong interest for an understanding of Quantum Chromodynamics (QCD). Charm and bottom quarks have masses significantly above the QCD scale, Λ_{QCD}, and hence low energy hadronization effects should not influence the total cross section and the distributions of the charm and bottom hadrons. In this approximation, properties of the jets containing heavy flavour hadrons are ex-

pected to be described accurately using perturbative calculations. A measurement of the production features of these jets can thus shed light on the details of the underlying QCD dynamics.

Several mechanisms contribute to heavy flavour quark production, such as quark-antiquark pair creation in the hard interaction or in the parton showering process. While the former is calculable in a perturbative approach, the latter may require additional non-perturbative corrections or different approaches such as a heavy quark mass expansion. In inclusive heavy flavour jet cross-sections, the contribution from gluon splitting in the final state parton showering could be identified by looking for two heavy flavour hadrons in a jet, but the different mechanisms for prompt heavy flavour quark production in the hard interaction remain indistinguishable. This complicates a comparison with theoretical calculations. A more exclusive study of the production of dijet events containing heavy flavour jets allows the different prompt heavy flavour quark creation processes to be separated, in addition to the gluon splitting contribution. For example, the dominant QCD production mechanisms are different for pairs of bottom flavour jets and pairs consisting of one bottom and one light jet. In this context, a measurement of the flavour composition of dijet events provides more detailed information about the different QCD processes involving heavy quarks.

The dijet system can be decomposed into six flavour states based on the contributing jet flavours. The jet flavour is defined by the flavour of the heaviest hadron in the jet. A light jet originates from fragmentation of a light flavour quark (u, d and s) or gluon and does not contain any bottom or charm hadrons. Three of these dijet states are the symmetric bottom+bottom ($b\bar{b}$), charm+charm ($c\bar{c}$) and light+light jet pairs. The three other combinations are the flavour-asymmetric bottom+light, charm+light and bottom+charm jet pairs. In the following discussion, these six dijet flavour

states will be denoted *BB*, *CC*, *UU*, *BU*, *CU*, *BC*, where *U* stands for light, *C* for charm and *B* for bottom jet.

Inclusive bottom jet and $b\bar{b}$ production in hadronic collisions have been studied by several experiments [1–5] in the past, see also a review [6] and references therein. Recently CMS published cross-sections for inclusive bottom jet production [7], $b\bar{b}$ decaying to muons [8] and bottom hadron production [9], as well as $B\bar{B}$ angular correlations [10]. The $b\bar{b}$ cross-section was also measured by LHCb [11]. ATLAS published a measurement of the $b\bar{b}$ cross-section in proton-proton collisions at $\sqrt{s} = 7$ TeV [12], employing explicit *b*-jet identification (*b*-tagging). However, the $b\bar{b}$ final state constitutes only a small fraction of the total heavy flavour quark production in dijet events, and the inclusive bottom cross-section contains a significant contribution from multi-jet states. This paper presents a simultaneous measurement of all six dijet flavour states, including those with charm. The *BC*, *CC* and *CU* dijet production at the LHC is studied for the first time. This approach provides more detailed information about the contributing QCD processes and challenges the theoretical description of the underlying dynamics employed in QCD Monte Carlo simulations.

The analysis procedure exploits reconstructed secondary vertices inside jets. Since kinematic properties of secondary vertices depend on the jet flavour, a measurement of the individual contributions of each flavour can be made by employing a fit using templates of kinematic variables. No explicit *b*-tagging is used, i.e. no flavours are assigned to individual jets. The excellent separation of charm and bottom flavoured jets in the ATLAS detector is demonstrated in the analysis.

The analysis uses the data sample collected by ATLAS at $\sqrt{s} = 7$ TeV in 2010, corresponding to an integrated luminosity of 39 pb^{-1}. The prescale settings of the different single-jet triggers used in the analysis varied with luminosity such that the actual recorded luminosity is dependent on the transverse momentum p_{T} of the leading jet.

This paper is organised as follows. The ATLAS detector is briefly described in Sect. 2. Section 3 describes the event and jet selection procedure for data and Monte Carlo simulation. Section 4 summarises the Monte Carlo simulation. Section 5 discusses the theoretical predictions for the flavour composition of dijet events. The reconstruction of secondary vertices in jets as well as the kinematic templates for the flavour analysis are presented in Sect. 6. A detailed account of the analysis method is given in Sect. 7. In Sect. 8 the results of the analysis are presented and systematic uncertainties are discussed.

2 The ATLAS detector

The ATLAS detector [13] was designed to allow the study of a wide range of physics processes at LHC energies. It consists of an inner tracking detector, surrounded by an electromagnetic calorimeter, hadronic calorimeters and a muon spectrometer. For the measurements presented in this paper, the tracking devices, the calorimeters and the trigger system are of particular importance.

The innermost detector, the tracker, is divided into three parts: the silicon pixel detector, the closest layer lying 5.05 cm from the beam axis, the silicon microstrip detector and the transition radiation tracker, with the outermost layer situated at 1.07 m from the beam axis. These offer full coverage in the azimuthal angle ϕ and a coverage in pseudorapidity of $|\eta| < 2.5$ [1]. The tracker is surrounded by a solenoidal magnet of 2 T, which bends the trajectories of charged particles so that their transverse momenta can be measured. The liquid argon and lead electromagnetic calorimeter covers a pseudorapidity range of $|\eta| < 3.2$. It is surrounded by the hadronic calorimeters, made of scintillator tiles and iron in the central region ($|\eta| < 1.7$) and of copper/tungsten and liquid argon in the endcaps ($1.5 < |\eta| < 3.2$). A forward calorimeter extends the coverage to $|\eta| < 4.9$. The muon spectrometer comprises three layers of muon chambers for track measurements and triggering. It uses a toroidal magnetic field with a bending power of 1–7.5 Tm and provides precise tracking information in a range of $|\eta| < 2.7$.

The ATLAS trigger system [13] uses three consecutive levels: level 1 (L1), level 2 (L2) and event filter (EF). The L1 triggers are hardware-based and use coarse detector information to identify regions of interest, whereas the L2 triggers are based on fast online data reconstruction algorithms. Finally, the EF triggers use offline data reconstruction algorithms. This study uses single-jet triggers.

3 Event and jet selection

Selected events are required to have at least one reconstructed primary vertex candidate. A candidate vertex must have at least 10 tracks with transverse momentum $p_{\mathrm{T}} > 150$ MeV associated to it, to ensure the quality of the vertex fit. If several vertex candidates are reconstructed, the one with the largest sum of the squared transverse momenta of associated tracks is considered to be the main interaction vertex and used as the primary vertex in the following.

Jets are reconstructed using the anti-k_t algorithm with a jet radius parameter $R = 0.4$ [14]. Topological clusters of energy deposits in the calorimeters are used as input for the clustering algorithm. Tracks within a cone of $\Delta R =$

---

[1]ATLAS uses a right-handed coordinate system with its origin at the nominal interaction point (IP) in the centre of the detector and the *z*-axis along the beam pipe. The *x*-axis points from the IP to the centre of the LHC ring, and the *y*-axis points upward. Cylindrical coordinates (r, ϕ) are used in the transverse plane, ϕ being the azimuthal angle around the beam pipe. The pseudorapidity is defined in terms of the polar angle θ as $\eta = -\ln\tan(\theta/2)$.

Leading jet p_T [GeV]	40–60	60–80	80–120	120–160	160–250	250–500
Subleading jet p_T [GeV]	30–60	40–80	50–120	75–160	100–250	140–500
Number of events	304103	251406	887185	660168	242979	146117
$\int L dt$ [nb^{-1}]	70	247	1880	8640	8640	38700

Table 1 Kinematic boundaries, together with the numbers of selected dijet events and the corresponding integrated luminosities for each leading jet p_T bin.

$\sqrt{(\Delta\varphi)^2 + (\Delta\eta)^2} = 0.4$ around the jet axis are assigned to the jet. Only jets with a transverse momentum of $p_T > 30$ GeV and a rapidity of $|y| < 2.1$ are considered. Jets in this rapidity range are fully contained in the tracker acceptance region, such that track and vertex reconstruction inside jets are not affected by the boundaries of the tracker acceptance. Jets are furthermore required to pass a quality selection [15, 16] that removes jets mimicked by noisy calorimeter cells or those that stem from non-collision backgrounds. Finally, the two jets with highest p_T in the analysis acceptance are required to have an angular separation in azimuth of $\Delta\varphi > 2.1$ rad, i.e. to be consistent with a back-to-back topology. This cut removes events in which one of the leading jets is produced by final-state hard gluon emission or jet splitting in the reconstruction.

The full data sample is split into six bins in the transverse momentum p_T of the leading jet. The bin boundaries correspond to the 99 % efficiency thresholds of the various single-jet triggers [17]. For events passing the trigger requirement, the leading and subleading jets have to fulfil pairwise-specific p_T conditions that are summarised in Table 1. The numbers of events selected in each leading jet p_T bin are shown in Table 1, together with the corresponding integrated luminosities.

4 Monte Carlo simulation

Dijet events are simulated using PYTHIA 6.423 [18] for the baseline template construction, parameter estimation and Monte Carlo (MC) comparisons. This leading-order (LO) generator is based on parton matrix-element calculations for $2 \rightarrow 2$ processes and a string hadronisation model. Modified leading-order MRST LO* [19] parton distribution functions are used in the simulation. Samples of dijet events were generated using a specific set of generator parameters, known as the ATLAS Minimum Bias Tune 1 (AMBT1) [20].

For the study of systematic effects and for the interpretation of the final results, other Monte Carlo samples are utilised. The main cross-check study is performed using the Herwig++ 2.4.2 [21] generator. The other LO samples used are PYTHIA with the next-to-leading-order (NLO) CTEQ 6.6 [22] parton distribution functions and Herwig 6.5 [23] used with JIMMY 4 [24, 25] for the simula-

tion of multiple parton interactions, using a specific ATLAS Underlying Event Tune (AUET1) [26]. The possible influence of multiple proton-proton interactions within the same bunch crossing is studied by adding minimum bias events, customised to the beam conditions of the 2010 LHC run at 7 TeV, to each PYTHIA event.

The PYTHIA 6.423+EVTGEN [27] event generator, using charm and bottom decay matrix elements with all sequential decay correlations and measured branching ratios, where available, is utilised for the simulation of the physics of bottom and charm hadron decays. It will be called PYTHIA+EVTGEN in the rest of the paper.

The NLO generator POWHEG [28–31] is used to interpret the analysis results. In POWHEG, the parton distribution function set used for the event generation is MSTW 2008 NLO [32] and the parton shower generator is PYTHIA.

In order to compare Monte Carlo predictions with data, "truth-particle" jets are used. They are defined by the anti-k_t $R = 0.4$ algorithm using only stable particles with a lifetime longer than 10 ps in the Monte Carlo event record. Muons and neutrinos do not contribute significantly to the jet energy in data. Therefore, they are also excluded from the truth-particle jets, to avoid having to correct for the missing jet energy in data.

The flavour of jets is assigned in the Monte Carlo simulation by labelling a jet as a b-jet if a bottom hadron with $p_T > 5$ GeV is found within a cone $\Delta R = 0.3$ around the jet axis. If no bottom hadron is present but a charm hadron is found using the same requirements, then the jet is labelled as a c-jet. All other jets are labelled as light jets. If two bottom hadrons with $p_T > 5$ GeV are found within a cone of size $\Delta R = 0.3$ the jet is labelled as a b-jet with two bottom hadrons, and similarly for c-jets with two charm hadrons.

The particle four-momenta are passed through the full simulation [33] of the ATLAS detector, which is based on GEANT4 [34]. The simulated events are reconstructed and selected using the same analysis chain as for data. After the dijet event selection, the Monte Carlo events are reweighted in each analysis p_T bin to match the observed leading and subleading jet p_T spectra. Any remaining discrepancies in the rapidity distributions between data and simulation are small and are included as sources of systematic uncertainty, as detailed in Sect. 8.3.
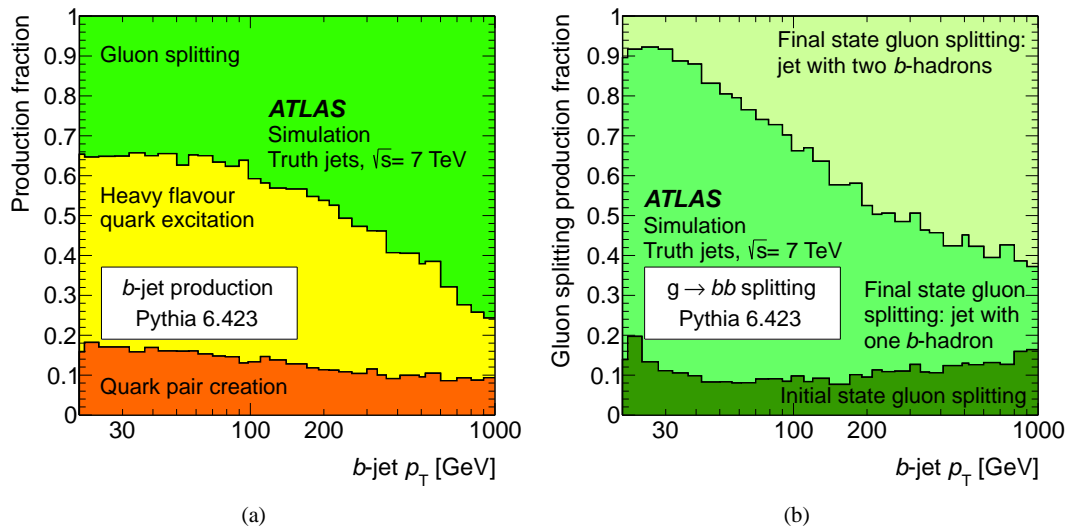
Fig. 1 The contributions of the different production processes to inclusive *b*-jet production in 7 TeV *pp* collisions are shown as a function of *b*-jet p_T, as given by PYTHIA 6.423 and obtained for truth-particle jets. The plot on the left (a) shows the contribution of quark pair creation, heavy flavour quark excitation and gluon splitting; the plot on the right (b) shows the different processes contributing to gluon splitting, namely initial- and final-state gluon splitting, the latter leading to jets with one or two *b*-hadrons. Truth-particle jets are reconstructed with the anti-k_t $R = 0.4$ algorithm in the $|y| < 2.1$ rapidity region.

5 Theoretical predictions

5.1 Heavy flavour production

Following the discussion in [35], heavy flavour quark production in hadronic collisions may be subdivided into three classes depending on the number of heavy quarks participating in the hard scattering. Hard scattering is defined as the $2 \to 2$ subprocess with the largest virtuality (or shortest distance) in the hadron-hadron interaction. In the following, *Q* stands for a heavy flavour quark, *q* for a light flavour quark and *g* for a gluon:

– *Quark pair creation*: two heavy quarks are produced in the hard subprocess. At leading order this is described by $gg \to Q\bar{Q}$ and $q\bar{q} \to Q\bar{Q}$.
– *Heavy flavour quark excitation*: a single heavy flavour quark from the sea of one hadron scatters against a parton from another hadron, denoted $gQ \to gQ$ and $qQ \to qQ$, respectively. Alternatively, the heavy flavour quark excitation process can be depicted as an initial-state gluon splitting into a heavy quark pair, where one of the heavy quarks subsequently enters the hard subprocess.
– *Gluon splitting*: in this case heavy quarks do not participate in the hard subprocess at all, but are produced in $g \to Q\bar{Q}$ branchings in the parton shower.

The relative contributions of the different heavy flavour quark production mechanisms to inclusive *b*-jet production are shown in Fig. 1(a) for simulated proton-proton collisions at 7 TeV. The fractions are calculated for anti-k_t jets in a ra-

pidity range of $|y| < 2.1$ with the PYTHIA 6.423 [18] generator. Figure 1(b) shows the decomposition of the gluon splitting process into initial- and final-state gluon splitting, the latter leading to jets with one or two *b*-hadrons.

The above classification is not strict but can be used as a basis for gaining a qualitative understanding of the features of heavy flavour quark production. Pair creation of heavy flavour quarks gives an insight into perturbative QCD with massive quarks. The back-to-back requirement used in the analysis reduces the contribution of NLO QCD effects to the jet-pair cross-sections with two heavy flavour jets, *BB* and *CC*. The heavy flavour quark excitation process, on the other hand, is sensitive to the heavy flavour components of the parton distribution functions of the proton. It produces mainly flavour asymmetric *BU* and *CU* jet pairs. The gluon splitting mechanism is sensitive to non-perturbative QCD dynamics and also contributes significantly to the mixed flavour jet pair states, i.e. *BU* and *CU*. However, this contribution is different from heavy flavour quark excitation because it creates a heavy quark-antiquark pair. The jet reconstruction algorithm either includes both heavy quarks in a single jet or misses one of them, thus reducing the reconstructed jet energy and its fraction taken by the remaining quark. The two possibilities result in different kinematic properties of the reconstructed secondary vertices in these jets, which can be exploited for the separation of gluon splitting from the heavy flavour quark excitation contribution.

To compare the predictions of theoretical models with data, the truth-particle jets defined in Section 4 are used in the analysis. The truth-particle dijet system is defined as the
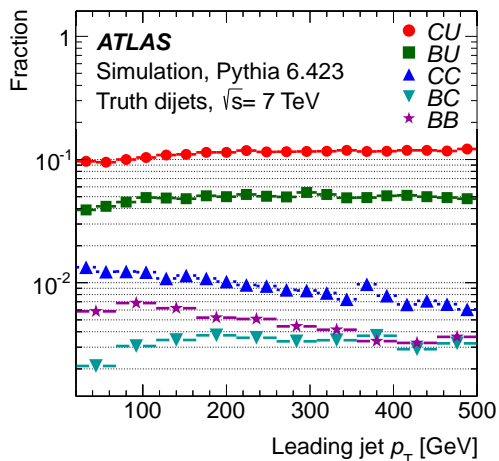
Fig. 2 PYTHIA 6.423 predictions for different bottom and charm dijet fractions as a function of leading jet p_T, obtained for truth-particle jet pairs, where the jets are back-to-back and have $p_T > 20$ GeV in the $|y| < 2.1$ rapidity region.

two truth-particle jets with the highest p_T in the $|y| < 2.1$ rapidity range, required to be consistent with a back-to-back topology, $\Delta\varphi > 2.1$ rad, with both the leading and subleading jets having $p_T > 20$ GeV.

The leading-order predictions for flavour jet production in truth-particle dijet events are illustrated in Fig. 2, where the ratio of different heavy+heavy and heavy+light dijet cross-sections to the total dijet cross-section is shown for $|y| < 2.1$ as a function of leading jet p_T, for 7 TeV pp collisions as predicted by PYTHIA 6.423. Heavy flavour jets in the dijet system are mainly produced in the *BU* and *CU* combinations. PYTHIA 6.423 predicts a slow decrease of the *BB* and *CC* fractions and an increase of the *BU* and *CU* jet fractions as a function of the leading jet p_T. The mixed *BC* fraction increases with jet p_T and becomes equal to the *BB* fraction above ~ 350 GeV.

5.2 Differences in heavy flavour rates in leading and subleading jets

The kinematic properties of the partons produced in hadronic interactions are mostly flavour independent, if mass effects are neglected. The two back-to-back partons with the highest p_T in the event should therefore not show any significant flavour-dependent difference in their kinematic features. However, the partons can be studied only through the corresponding jet properties after hadronisation. Heavy flavour quark presence in a jet can influence the jet properties through the following mechanisms:

– Semileptonic decays of heavy flavour hadrons decrease the jet energy, because neutrinos are not detected and the muon energy is not measured in the calorimeter. This

energy loss is absent for light jets and is very different for bottom and charm jets.
– If several heavy flavour quarks appear in the jet fragmentation process (e.g. via gluon splitting) one of them can be left outside the jet volume by the jet reconstruction algorithm, which leads to a reduction in the jet energy.

As a result, the average jet energy for heavy flavours becomes smaller than the jet energy for light flavours, such that heavy flavour jets are predominantly produced as subleading jets in the mixed-flavour dijet pairs. This effect can be described using a flavour asymmetry defined as

$$A_{b,c} = \frac{N_{b,c}^{SL}}{N_{b,c}^{L}} - 1, \tag{1}$$

where $N_{b,c}^{L,SL}$ denote the number of leading or subleading bottom or charm jets. The predictions for $A_{b,c}$ given by different Monte Carlo generators are shown in Fig. 3 for the truth particle jets defined in Sect. 4.
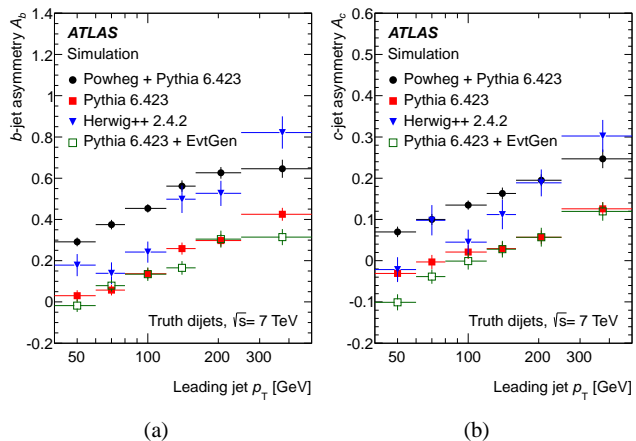

Fig. 3 The asymmetries in the amount of (a) bottom and (b) charm truth particle jets as taken from POWHEG+PYTHIA 6.423 (black points), PYTHIA 6.423 (squares), Herwig++ 2.4.2 (triangles) and PYTHIA+EVTGEN (open squares) in leading and subleading jets, for each leading jet p_T bin used in the analysis.

POWHEG, which includes higher-order QCD effects, predicts a significant flavour asymmetry which increases strongly with jet p_T. The flavour asymmetry predictions of the LO PYTHIA generator are smaller than those of the NLO POWHEG generator. The latter uses PYTHIA 6.423 for the fragmentation and thus shares the same description of the decays of heavy flavour hadrons. Since the influence of the different parton distribution functions was also found to be negligible, the differences in $A_{b,c}$ between these generators (Fig. 3) should be attributed primarily to NLO QCD effects. The LO Herwig++ generator employs another fragmentation model and predicts asymmetries similar to the POWHEG ones, although with a somewhat different p_T dependence.

For the measurement of the dijet flavour fractions, this flavour asymmetry needs to be correctly described in the data analysis. The fact that the Monte Carlo generators predict significantly different asymmetries indicates that $A_{b,c}$ should be determined directly from the data.

6 Secondary vertex reconstruction and analysis templates

Secondary vertices are displaced from the primary vertex because they originate from the decays of long-lived particles. Kinematic properties of these vertices, e.g. the invariant mass or total energy of the outgoing particles, depend on the corresponding properties of the original heavy flavour hadrons and are therefore different for bottom and charm jets. Reconstructed secondary vertices in light jets are mainly due to K_S^0 and Λ [36] decays, interactions in the detector material, or fake vertices. The fake reconstructed vertices are composed of tracks which occasionally get close together due to a high density of tracks in the jet core and track reconstruction errors. Their properties are very different from those of heavy flavour decays. The current analysis exploits these differences by combining the kinematic features of the reconstructed secondary vertices in an optimal way into templates for bottom, charm and light jets.

6.1 Secondary vertex reconstruction in jets

The vertex reconstruction algorithm aims at a high reconstruction efficiency and therefore determines vertices in an inclusive way, i.e. a single secondary vertex is fitted for each jet. In the case of a bottom hadron decay, the subsequent charm hadron decay vertex is usually close to the bottom one and is therefore not reconstructed separately. A detailed discussion of the algorithm and its performance can be found in the b-tagging chapter of Ref. [17]. The reconstruction starts by combining pairs of good quality tracks inside jets to make vertices, where the latter are required to be displaced significantly from the primary interaction vertex. The two-track vertices coming from K_S^0 and Λ decays and interactions in the detector material are removed from further consideration. For the light jets, the remaining candidates after this cleaning are mainly fake vertices. All remaining two-track vertices are merged into a single vertex. This vertex is refitted iteratively by removing tracks until a good vertex fit quality is obtained. The corresponding decay length is defined as a signed quantity, where the sign is fixed by the projection of the decay length vector—the vector pointing from the primary event vertex to the secondary vertex—onto the jet axis. The vertex is required to have a positive decay length and a total invariant mass, calculated using the

momenta of associated particles and assigning them pion masses [36], greater than 0.4 GeV.

6.2 Secondary vertex reconstruction efficiencies

The secondary vertex reconstruction efficiency is dependent on the jet p_T due to several effects such as the p_T dependence of the track reconstruction accuracy and the increase of the flight distance of heavy flavour hadrons with growing jet p_T. The probability of reconstructing a fake vertex in a light jet is also affected by the increase of the number of tracks in a jet with jet p_T. Due to the p_T-dependent vertex efficiency and different p_T distributions for leading and subleading jets in dijet pairs, the number of reconstructed secondary vertices in these jets are different.

The secondary vertex reconstruction efficiencies predicted by the ATLAS detector simulation based on dijet events from PYTHIA 6.423 are shown in Fig. 4. There is no difference between secondary vertex reconstruction efficiencies in leading and subleading jets for charm and bottom jets. However, the fake vertex reconstruction probability in light jets is noticeably higher for subleading jets. This requires the introduction of two separate secondary vertex probabilities for leading and subleading light jets.

6.3 Template construction and features

The specific choice of the kinematic variables for the dijet flavour measurement is driven by the requirement to have maximal sensitivity to the flavour content. Furthermore, if several variables are to be used, the correlations between them should be kept small. Another important requirement is a minimal dependence on the jet p_T and rapidity, in order to minimise systematic effects due to a possible p_T or rapidity mismatch between data and Monte Carlo simulation. Also, p_T-invariant variables allow a robust analysis to be made over a wide range of p_T.

For this study the following two variables are chosen:

$$\Pi = \frac{m_\text{vertex} - 0.4\,\text{GeV}}{m_B} \cdot \frac{\sum\limits_\text{vertex} E_i}{\sum\limits_\text{jet} E_i} \tag{2}$$

$$B = \frac{\sqrt{m_B} \cdot \sum\limits_\text{vertex} |\vec{p}_{\text{T}i}|}{m_\text{vertex} \cdot \sqrt{p_{\text{T}jet}}}, \tag{3}$$

where each sum indicates whether the summation is performed over particles associated with the secondary vertex, or over all charged particles in the jet. Particle transverse momentum and energy are denoted as p_T and E, respectively. In essence, Π is the product of the invariant mass of the particles associated with the vertex (m_vertex) and the energy fraction of these particles with respect to all charged
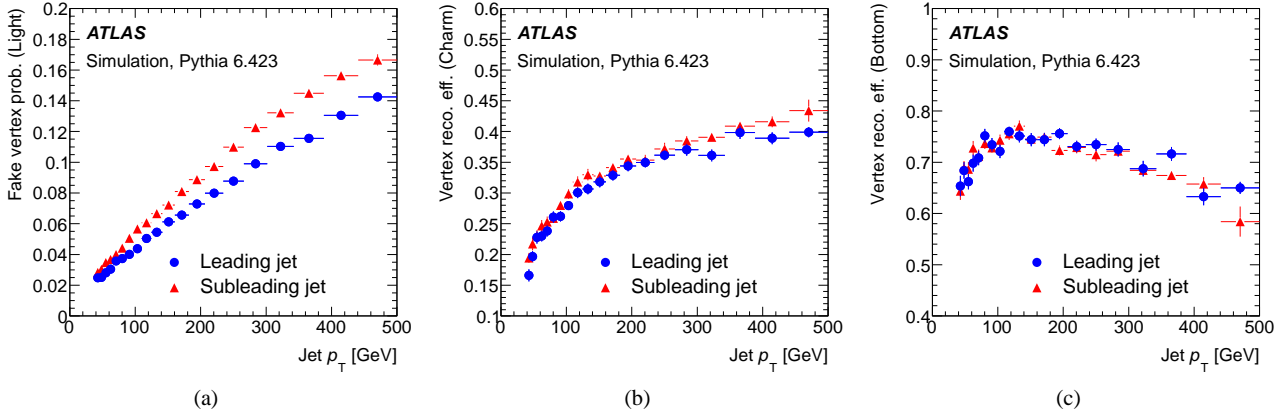
Fig. 4 The reconstruction probabilities for fake vertices in (a) light jets, as well as the reconstruction efficiencies for secondary vertices in (b) charm and (c) bottom jets, are displayed as a function of the jet p_T as predicted by PYTHIA 6.423.
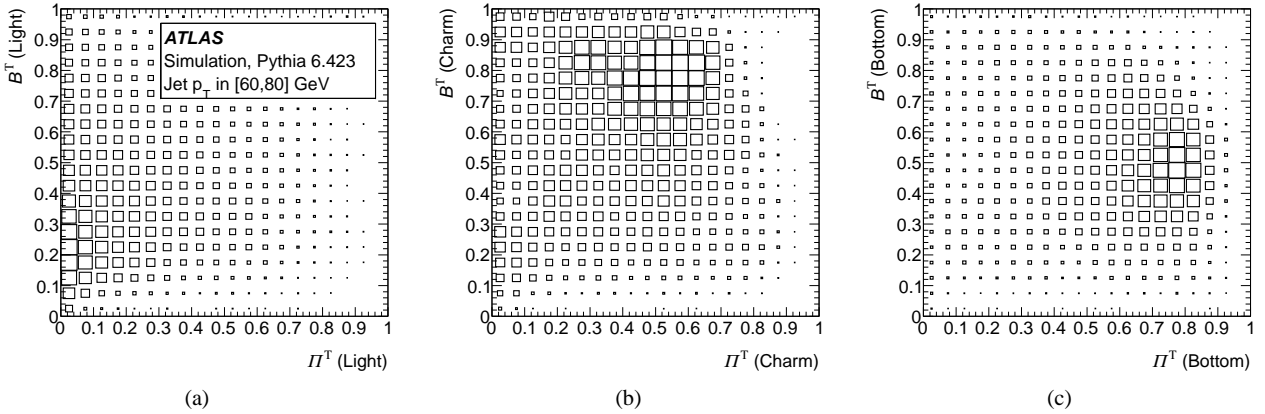

Fig. 5 Two-dimensional distributions of $\Pi^\top$ and $B^\top$ (flavour templates) obtained with PYTHIA 6.423 for (a) light, (b) charm and (c) bottom jets with p_T in the bin $[60, 80]$ GeV.

particles in the jet. The 0.4 GeV constant in Eq.(2) is the cut value used for the secondary vertex selection in this analysis. The parameter B corresponds approximately to the relativistic γ factor of the system composed of the particles associated with the vertex, normalised to the square root of the jet transverse momentum. The $m_B = 5.2794$ GeV constant is the average B-meson mass [36] and is used for normalisation.

To facilitate the fit procedure, the variables are transformed into the interval $[0,1]$:

$$\Pi^\top = \frac{\Pi}{\Pi + 0.04} \tag{4}$$

$$B^\top = \frac{B \cdot B}{B \cdot B + 10}. \tag{5}$$

The tuning constants 0.04 in Eq.(4) and 10 in Eq.(5) have been chosen to maximise the difference in the mean values between the light and heavy flavour distributions.

Joint distributions of these observables are shown in Fig. 5 for light, charm and bottom jets in the $[60, 80]$ GeV

bin, as predicted by the full detector simulation of PYTHIA 6.423 events. These two-dimensional distributions are used as flavour templates $U(\Pi^\top, B^\top)$, $C(\Pi^\top, B^\top)$ and $B(\Pi^\top, B^\top)$ in the analysis as detailed in Section 7. Features of the observables are also illustrated in Figs. 6 and 7. Both $\Pi^\top$ and $B^\top$ are independent of jet rapidity for all jet flavours. This is illustrated in Fig. 6 for the light jet templates, which are most sensitive to reconstruction and detector effects. The $\Pi^\top$ variable is very similar in shape in the $[40, 60]$ GeV and $[250, 500]$ GeV bins and is only weakly p_T-dependent. Figure 7 demonstrates that $\Pi^\top$ is only weakly dependent on the different heavy flavour production mechanisms described in Sect. 5. In contrast, the $B^\top$ variable is sensitive to the gluon splitting contribution, in particular to the case where this mechanism produces two quarks of the same flavour in a jet. In addition $B^\top$ has a distinct p_T dependence. However, the $B^\top$ variable provides good sensitivity to the charm contribution. No difference in flavour templates between leading and subleading jets is observed.
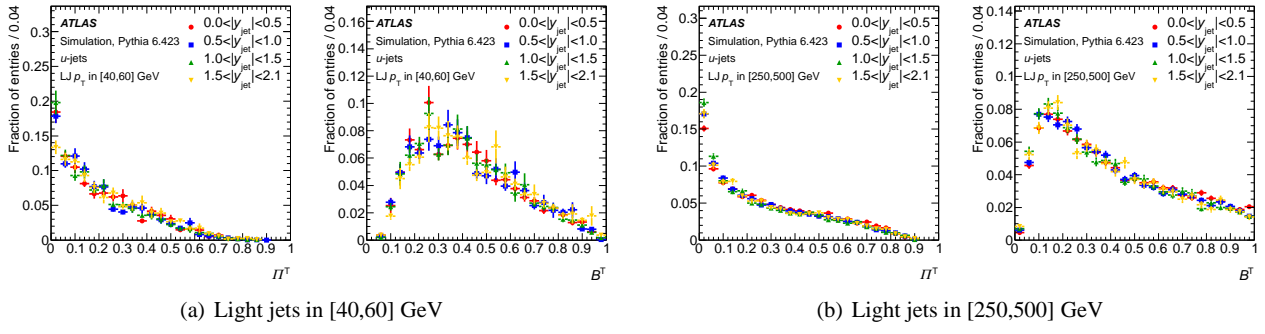
(a) Light jets in [40,60] GeV

(b) Light jets in [250,500] GeV

Fig. 6 The $\Pi^\top$ and $B^\top$ distributions of light jets in the (a) $[40, 60]$ GeV and (b) $[250, 500]$ GeV leading jet (LJ) p_T analysis bins obtained with fully simulated PYTHIA 6.423 dijet events. The distributions are shown in different jet rapidity ranges.
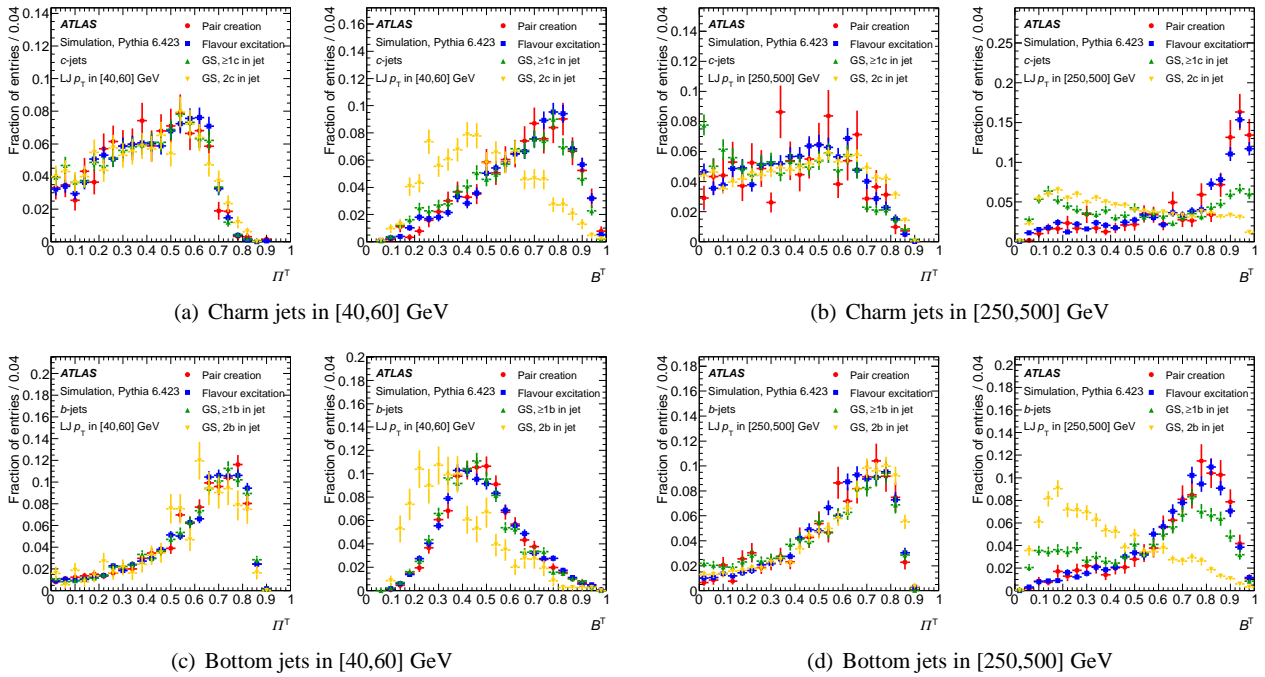

(a) Charm jets in [40,60] GeV

(b) Charm jets in [250,500] GeV

(c) Bottom jets in [40,60] GeV

(d) Bottom jets in [250,500] GeV

Fig. 7 The $\Pi^\top$ and $B^\top$ distributions in the $[40, 60]$ GeV leading jet (LJ) p_T range for (a) charm jets and (c) bottom jets as well as in the $[250, 500]$ GeV range for (b) charm jets and (d) bottom jets obtained with fully simulated PYTHIA 6.423 dijet events. The distributions are shown separately for jets stemming from quark pair creation, heavy flavour quark excitation, gluon splitting (GS) with one or two heavy flavour quarks inside the jet. All distributions are normalised separately to unit area.

The fraction of jets with two heavy quarks produced in gluon splitting may be incorrectly predicted by the PYTHIA simulation, especially in the high p_T region where this contribution becomes large (see Fig. 1). This phenomenon was discussed in more detail in [37]. Therefore a separate contribution of doubly-flavoured jets is included in the analysis, to account for the corresponding dependence of the $B^\top$ variable. The two-dimensional template for bottom jets is replaced by the two-component template

$$B(\Pi^\top, B^\top) \to (1 - b_2) \cdot B(\Pi^\top, B^\top) + b_2 \cdot B_2(\Pi^\top, B^\top), \quad (6)$$

where $B_2(\Pi^\top, B^\top)$ is a template for jets with two b-hadrons and b_2 is a parameter governing the deviation from the de-

fault 2b-jet $B(\Pi^\top, B^\top)$ content provided by PYTHIA 6.423. The charm jet template is modified similarly with substitutions $b_2 \to c_2$ and $B_2(\Pi^\top, B^\top) \to C_2(\Pi^\top, B^\top)$. Using Eq.(6), the heavy flavour template shapes can be obtained directly from the data by optimising the b_2 and c_2 parameters to achieve the best possible data description. As is demonstrated in Sect. 8, the adjustment of the contribution of jets with two b-hadrons to the bottom template significantly improves the overall quality of the description of the dijet data.

6.4 Template tuning on data using track impact parameters

The secondary vertex reconstruction algorithm uses track impact parameters divided by their measurement uncertainties for the vertex search, thus its results depend crucially on the track impact parameter resolution. A good description of the track impact parameter accuracy and the corresponding covariance matrix is therefore mandatory in the detector simulation, in order for the secondary vertex templates to be constructed correctly.

To improve the agreement between data and Monte Carlo simulation, the analysis templates are tuned on data. Firstly, an additional track impact parameter smearing is applied to the PYTHIA events. To estimate the necessary amount of smearing, the data and Monte Carlo track impact parameter distributions are compared in bins of track p_T and pseudorapidity [38]. However, the smearing procedure does not correct the track covariance matrices. A second step is therefore taken. Two sets of templates are produced, using both the smeared and non-smeared PYTHIA 6.423 samples. A normalised mixture is then compared with the data, using secondary vertices with negative decay length to obtain the optimal mixing fraction. These vertices depend only weakly on the exact flavour content of jets and are not used in the dijet analysis. The mixing fraction is chosen to be flavour independent. The optimal description of the data for the full p_T range is obtained with a fraction $F_{smear} = 0.654 \pm 0.023$ for the smeared template in the mixture. This template tuning procedure gives a significant improvement in the data fit quality in the signal region.

7 Analysis method

7.1 Dijet system description

The secondary vertex reconstruction procedure can find vertices with probabilities v_U, v_C and v_B for light, charm and bottom jets, respectively. For simplicity, the p_T-dependence of these probabilities and the differences between leading and subleading jets (see Sect. 6.2) are neglected for the moment. In the leading and subleading jet of a dijet event, zero, one or two secondary vertices can be reconstructed overall. The numbers of 2-, 1-, or 0-vertex dijet events can be calculated as:

$$\frac{N_{2V}}{N} = v_U v_U f_{UU} + v_C v_C f_{CC} + v_B v_B f_{BB} \tag{7}$$
$$+ v_U v_C f_{CU} + v_U v_B f_{BU} + v_C v_B f_{BC}$$

$$\frac{N_{1V}}{N} = 2(1 - v_U) \cdot v_U \cdot f_{UU} + 2(1 - v_C) \cdot v_C \cdot f_{CC} \tag{8}$$
$$+ 2(1 - v_B) \cdot v_B \cdot f_{BB}$$
$$+ ((1 - v_U) \cdot v_C + v_U \cdot (1 - v_C)) \cdot f_{CU}$$
$$+ ((1 - v_U) \cdot v_B + v_U \cdot (1 - v_B)) \cdot f_{BU}$$
$$+ ((1 - v_C) \cdot v_B + v_C \cdot (1 - v_B)) \cdot f_{BC}$$

$$N_{0V} = N - N_{1V} - N_{2V}. \tag{9}$$

Here N is the total number of dijet events and f_{XX} is the fraction of the respective dijet flavour component chosen such that

$$f_{UU} + f_{CC} + f_{BB} + f_{CU} + f_{BU} + f_{BC} = 1. \tag{10}$$

The joint distribution of the $\Pi^\top$ and $B^\top$ variables for dijet events with one reconstructed secondary vertex can be obtained using Eq.(8):

$$\mathscr{D}(\Pi^\top, B^\top) = 2(1 - v_U) v_U f_{UU} U(\Pi^\top, B^\top) \tag{11}$$
$$+ 2(1 - v_C) v_C f_{CC} C(\Pi^\top, B^\top)$$
$$+ 2(1 - v_B) v_B f_{BB} B(\Pi^\top, B^\top)$$
$$+ \left\{ (1 - v_U) v_C C(\Pi^\top, B^\top) + v_U(1 - v_C) U(\Pi^\top, B^\top) \right\} f_{CU}$$
$$+ \left\{ (1 - v_U) v_B B(\Pi^\top, B^\top) + v_U(1 - v_B) U(\Pi^\top, B^\top) \right\} f_{BU}$$
$$+ \left\{ (1 - v_C) v_B B(\Pi^\top, B^\top) + v_C(1 - v_B) C(\Pi^\top, B^\top) \right\} f_{BC}.$$

Here $\mathscr{D}(\Pi^\top, B^\top)$ is the observed data distribution and $U(\Pi^\top, B^\top)$, $C(\Pi^\top, B^\top)$ and $B(\Pi^\top, B^\top)$ are templates derived from Monte Carlo simulation with

$$\int U(\Pi^\top, B^\top) d\Pi^\top dB^\top = \int C(\Pi^\top, B^\top) d\Pi^\top dB^\top \tag{12}$$
$$= \int B(\Pi^\top, B^\top) d\Pi^\top dB^\top = 1.$$

The case of two reconstructed vertices requires more careful consideration. Assuming that the two jets are independent, the joint distribution of $\Pi^\top$ and $B^\top$ can be written considering Eq.(7) in the following way:

$$\mathscr{D}(\Pi_1^\top, B_1^\top, \Pi_2^\top, B_2^\top) = \tag{13}$$
$$v_U v_U f_{UU} \cdot U(\Pi_1^\top, B_1^\top) U(\Pi_2^\top, B_2^\top)$$
$$+ v_C v_C f_{CC} \cdot C(\Pi_1^\top, B_1^\top) C(\Pi_2^\top, B_2^\top)$$
$$+ v_B v_B f_{BB} \cdot B(\Pi_1^\top, B_1^\top) B(\Pi_2^\top, B_2^\top)$$
$$+ 0.5 \cdot v_U v_C f_{CU}$$
$$\times \left\{ U(\Pi_1^\top, B_1^\top) C(\Pi_2^\top, B_2^\top) + U(\Pi_2^\top, B_2^\top) C(\Pi_1^\top, B_1^\top) \right\}$$
$$+ 0.5 \cdot v_U v_B f_{BU}$$
$$\times \left\{ U(\Pi_1^\top, B_1^\top) B(\Pi_2^\top, B_2^\top) + U(\Pi_2^\top, B_2^\top) B(\Pi_1^\top, B_1^\top) \right\}$$
$$+ 0.5 \cdot v_C v_B f_{BC}$$
$$\times \left\{ C(\Pi_1^\top, B_1^\top) B(\Pi_2^\top, B_2^\top) + C(\Pi_2^\top, B_2^\top) B(\Pi_1^\top, B_1^\top) \right\}.$$

Provided that the templates $U(\Pi^\top, B^\top)$, $C(\Pi^\top, B^\top)$ and $B(\Pi^\top, B^\top)$ are given, the eight variables

v_U, v_C, v_B, f_{CC}, f_{BB}, f_{BU}, f_{CU}, f_{BU} fully describe the properties of secondary vertices in ideal dijet events without kinematic dependencies. Note that only five fractions are needed, since any of the six fractions depends on the others through Eq.(10). In this paper the quantity f_{UU} is excluded.

The description of the dijet system must be modified to take into account the dijet flavour asymmetry (Sect. 5.2). The *BB* and *CC* dijet states are flavour-symmetric and thus do not require any modifications in their treatment. The description of the *BC* dijet fraction is also left symmetric because charm and bottom asymmetries partially compensate each other and the fraction itself is small ($\leq 0.5\%$). Thus only the treatment of the *BU* and *CU* fractions has to be modified. The analysis formalism is changed in the following way. The sample of dijet events with only one reconstructed secondary vertex is split into two subsamples, according to whether the vertex is reconstructed in the leading or subleading jet. These two subsamples are described separately, assuming different contributions of the *CU* and *BU* dijet fractions. More specifically, the f_{CU} and f_{BU} coefficients in Eq.(8) and Eq.(11) are replaced by pairs of coefficients f_{CU}^L, f_{CU}^{SL} and f_{BU}^L, f_{BU}^{SL} for leading and subleading jets, respectively. *L* and *SL* denote here whether the heavy flavour is in the leading or in the subleading jet. The jet flavour asymmetry of Eq.(1) can be rewritten as $A_{b,c} = f_{\{B,C\}U}^{SL}/f_{\{B,C\}U}^L - 1$. The new equations for events with a reconstructed secondary vertex in the leading jet can then be written:

$$\frac{N_{1V}^L}{N^L} = 2 \cdot (1-v_U) \cdot v_U \cdot f_{UU} + 2 \cdot (1-v_C) \cdot v_C \cdot f_{CC} \quad (14)$$
$$+ 2 \cdot (1-v_B) \cdot v_B \cdot f_{BB}$$
$$+ (1-v_U) \cdot v_C \cdot f_{CU}^L + v_U \cdot (1-v_C) \cdot f_{CU}^{SL}$$
$$+ (1-v_U) \cdot v_B \cdot f_{BU}^L + v_U \cdot (1-v_B) \cdot f_{BU}^{SL}$$
$$+ ((1-v_C) \cdot v_B + v_C \cdot (1-v_B)) \cdot f_{BC}$$

$$\mathscr{D}^L(\Pi^\top, B^\top) = 2 \cdot (1-v_U) v_U f_{UU} \cdot U(\Pi^\top, B^\top) \quad (15)$$
$$+ 2 \cdot (1-v_C) v_C f_{CC} \cdot C(\Pi^\top, B^\top)$$
$$+ 2 \cdot (1-v_B) v_B f_{BB} \cdot B(\Pi^\top, B^\top)$$
$$+ (1-v_U) v_C \cdot C(\Pi^\top, B^\top) f_{CU}^L + v_U (1-v_C) \cdot U(\Pi^\top, B^\top) f_{CU}^{SL}$$
$$+ (1-v_U) v_B \cdot B(\Pi^\top, B^\top) f_{BU}^L + v_U (1-v_B) \cdot U(\Pi^\top, B^\top) f_{BU}^{SL}$$
$$+ \left\{ (1-v_C) v_B \cdot B(\Pi^\top, B^\top) + v_C (1-v_B) \cdot C(\Pi^\top, B^\top) \right\} f_{BC}.$$

The corresponding equations for dijet events with a reconstructed secondary vertex in the subleading jet can be obtained from Eq.(14) and Eq.(15) by substituting $f_{CU}^L \leftrightarrow f_{CU}^{SL}$ and $f_{BU}^L \leftrightarrow f_{BU}^{SL}$.

7.2 Data fitting function

The complete dijet model combines all the ingredients presented in the previous sections. The formulae above can be modified to take into account the dependence of the vertex reconstruction efficiencies on jet p_T, as well as on whether jets are leading or subleading (Sect. 6.2). Variable fractions of jets with two bottom or charm quarks inside can also be incorporated (Sect. 6.3). The full model has the following set of parameters:

$$v_U^L(p_T), v_U^{SL}(p_T), v_C(p_T), v_B(p_T), \quad (16)$$
$$f_{BB}, f_{BC}, f_{CC}, f_{BU}, f_{CU},$$
$$A_c, c_2, A_b, b_2.$$

In order to reduce the set of parameters in the model to the maximum that is affordable with the 2010 data statistics, additional assumptions need to be made. The charm and bottom vertex reconstruction efficiencies are defined mainly by heavy flavour hadron lifetimes and heavy parton fragmentation functions, which are known well from previous experiments. Therefore, Monte Carlo predictions for v_B and v_C are more robust than the fake vertex probability in light jets v_U, which is governed mainly by detector and reconstruction accuracies. The charm asymmetry A_c is smaller than the bottom one (Fig. 3) and the admixture of jets with two charm quarks influences the charm template shape less than in the bottom case (Fig. 7). Therefore, the following simplifications are used in the analysis:

- The fraction of jets with two charm quarks is set to the baseline PYTHIA 6.423 prediction.
- The charm jet asymmetry is fixed to $A_c = \max(0, A_c^{MC})$ using the PYTHIA 6.423 prediction, see Fig. 3.
- The p_T-dependent parameterisations obtained with the full ATLAS detector simulation (Fig. 4) are used for bottom and charm vertex reconstruction efficiencies $v_C(p_T) = v_C^{MC}(p_T)$ and $v_B(p_T) = v_B^{MC}(p_T)$.
- The light jet vertex reconstruction probabilities are parametrised as $v_U^L(p_T) = sv_U^L \cdot v_U^{L(MC)}(p_T)$ and $v_U^{SL}(p_T) = sv_U^{SL} \cdot v_U^{SL(MC)}(p_T)$ for leading and subleading jets, respectively. Here $v_U^{L(MC)}(p_T)$ and $v_U^{L(MC)}(p_T)$ are the p_T-dependent secondary vertex rates in light jets, obtained with the full detector simulation and shown in Fig. 4. The scaling factors sv_U^L, sv_U^{SL} are allowed to vary in the fit.

The final model has a reduced set of nine free parameters:

$$sv_U^L, sv_U^{SL}, f_{BB}, f_{BC}, f_{CC}, f_{BU}, f_{CU}, A_b, b_2. \quad (17)$$

This simplified model is used for fitting. Systematic effects originating from the simplifications above are included in the systematic uncertainties on the flavour fraction measurements.

7.3 Validation of the analysis method

A dedicated simulation technique was developed to validate the analysis method. It uses a set of secondary vertices, which are reconstructed in all jets in the dijet sample generated with PYTHIA after full ATLAS simulation, and are stored in a dedicated database in bins of jet p_T, rapidity and flavour.

To produce a dijet event, the p_T and $|y|$ values for each jet are generated randomly according to the corresponding data distributions. Jet flavours are assigned according to the predefined dijet flavour fractions and the flavour asymmetries (Sect. 5.2). The flavour-dependent vertex reconstruction efficiencies (Fig. 4) determine whether a secondary vertex is reconstructed in the generated jet. The vertex parameters are then taken from a fully simulated secondary vertex, picked at random from the vertex database bin with corresponding p_T and $|y|$.

Two independent sets of events are generated in a pseudo-experiment, one for the construction of templates and one to define a pseudo-data sample. These pseudo-data are analyzed, using the relevant templates, to estimate the model parameters. Repetition of the pseudo-experiments has demonstrated that the fit method is able to measure the model parameters in Eq.(17) within a wide range of initial values. The estimators obtained from the fits are unbiased and have pull distribution dispersions close to one.

8 Results

8.1 Data fit results

An event-based extended maximum likelihood fit is used to fit the data. The fit is performed using the MINUIT [39] package included in the ROOT [40] framework. A multinomial distribution is used in the likelihood function to describe the numbers of dijet events with zero, one or two reconstructed vertices. Using the MINUIT package, a detailed investigation of the likelihood function in the region around its maximum value has been performed, to estimate the statistical uncertainties. It has been found that the parabolic approximation of the analysis fitting function is valid around the maximum point.

The quality of the description of the data obtained with the fit is illustrated in Fig. 8, where the data are compared with the Monte Carlo distributions predicted by the fit in the [160, 250] GeV analysis bin. All features of the data distribution are correctly reproduced, with a relative accuracy of better than 10%. The residual differences are within the systematic uncertainties of the measurements.

Figure 9(a) presents the fitted vertex probability in light jets together with the prediction for dijet events generated with PYTHIA 6.423 and passing through the full detector simulation. The probability is averaged over leading and subleading jets in each p_T bin. The vertices found in light jets are mainly fake ones (Sect. 6), therefore their probability is very sensitive to the details of the track and vertex reconstruction. Good agreement between data and Monte Carlo simulation demonstrates that the ATLAS detector performance is well understood in the Monte Carlo simulation.

Figure 9(b) shows the deviation of the admixture of jets containing two bottom hadrons, b_2, from the PYTHIA 6.423 prediction. The significance of the measured admixture excess confirms the importance of this additional contribution of double-bottom jets for a correct description of the data. This observation agrees with the results of [37]. The double-bottom jets are produced by the gluon splitting mechanism (Sect. 5). However, the analysis is unable to determine if a contribution from this mechanism to the fraction of jets with a single bottom hadron (see Fig. 1(b)) is also enhanced in data.

The fit results for the b-jet asymmetry A_b need to be corrected for detector effects, in order to represent truth-particle jets. The necessary correction is defined as a difference between truth-particle jet and reconstructed jet asymmetries, averaged over all p_T bins using PYTHIA 6.423, Herwig++ 2.4.2 and PYTHIA+EVTGEN dijet events. The resulting correction of 0.08 ± 0.02 units is added to the fit results. The corrected b-jet asymmetry is compared to the truth-particle b-jet asymmetries in PYTHIA 6.423, POWHEG+PYTHIA 6.423 and Herwig++ 2.4.2 in Fig. 9(c). PYTHIA 6.423 predicts a much smaller b-jet asymmetry than observed in the data. Since semileptonic decays are well described in PYTHIA 6.423, the undetected energy due to neutrinos and muons from these decays cannot be the main contributor to the observed b-jet asymmetry. Modifications of the PYTHIA 6.423 generator, such as different proton structure functions or different bottom parton fragmentation functions, are unable to improve substantially the agreement between the data and Monte Carlo simulation. The b-jet asymmetry predicted by Herwig++ 2.4.2 grows faster with p_T than for the data. The best description of the data is provided by the POWHEG+PYTHIA 6.423 generator, suggesting that NLO accuracy is needed to reproduce the b-jet asymmetry reliably.

8.2 Unfolding

To allow for a comparison with theoretical predictions and to remove detector resolution and acceptance effects, the flavour fractions for data must be unfolded to the truth-particle jet level as defined in Sect. 5. A simple bin-by-bin correction method is used. The expected inaccuracy introduced by the unfolding procedure itself is small in comparison with the measurement uncertainties. The unfolding correction factors for each flavour combination and leading jet
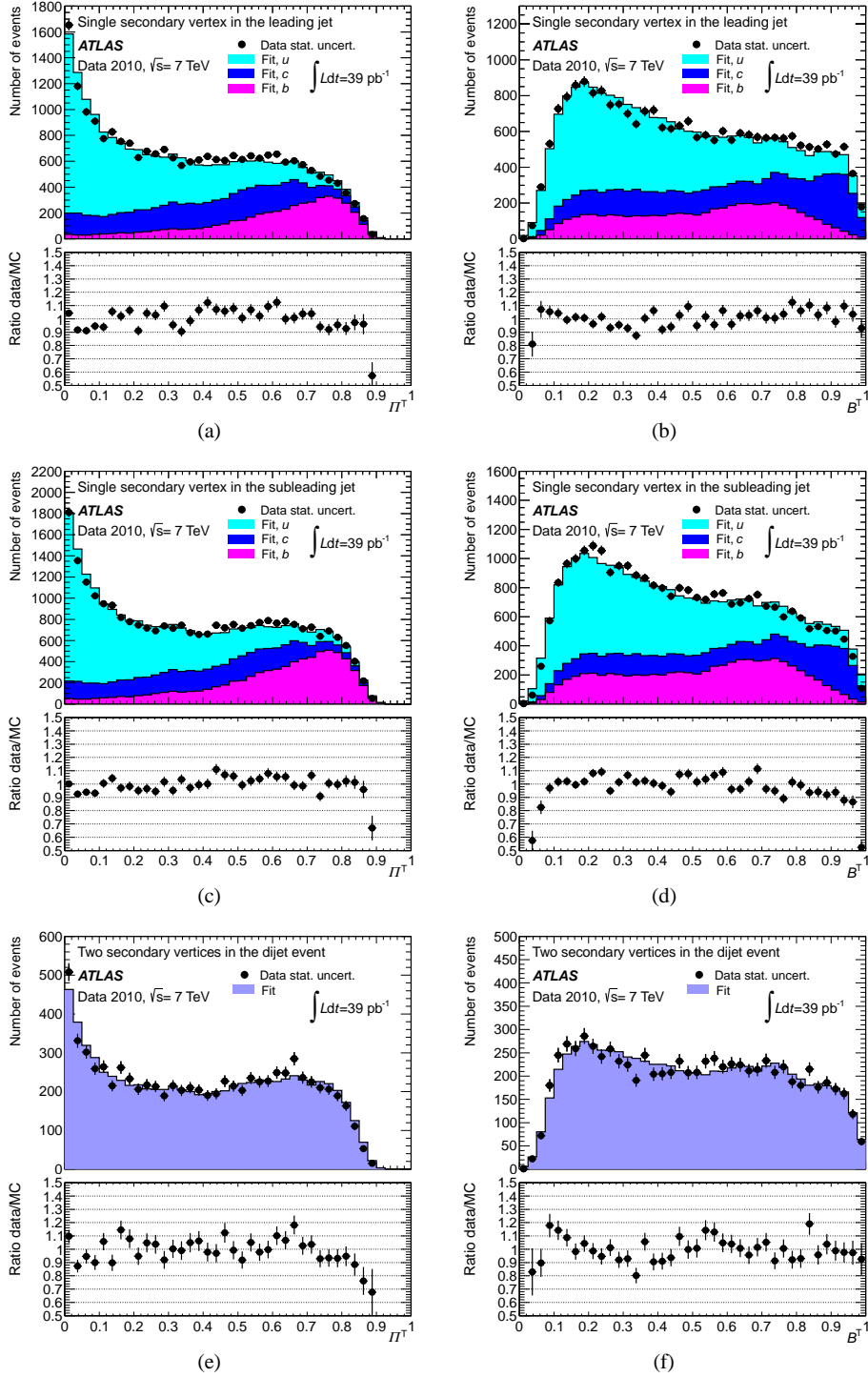
Fig. 8 Data description with the Monte Carlo templates obtained as a result of the fit in the $[160, 250]$ GeV analysis bin. (a) and (b) show the $\Pi^\top$ and $B^\top$ distributions for secondary vertices in the leading jet, (c) and (d) show the same distributions for secondary vertices in the subleading jet in events with a single secondary vertex in two jets. (e) and (f) show the $\Pi^\top$ and $B^\top$ distributions in the events with two secondary vertices averaged over leading and subleading jets. Data statistical uncertainties only are used to calculate the errors of the data to the Monte Carlo prediction ratios.

p_T bin are determined as ratios of the reconstructed dijet events with required jet flavours to the corresponding truth-particle dijet events (Sect. 5) in a given bin. They are calcu-

lated using the fully simulated PYTHIA 6.432 dijet sample and are typically in the 60%–100% range, mainly because of the p_T cut on the reconstructed subleading jet. The correc-

Fig. 9 Data fit results for the (a) average fake vertex probability in light jets v_u, (b) 2b-jet admixture deviation b_2 and (c) bottom dijet asymmetry A_b. Statistical uncertainties only are shown. The fake vertex probability is shown with the PYTHIA 6.423 reconstructed jet predictions. The 2b-jet admixture deviation parameter should be zero if PYTHIA 6.423 were fully consistent with data. The fitted bottom dijet 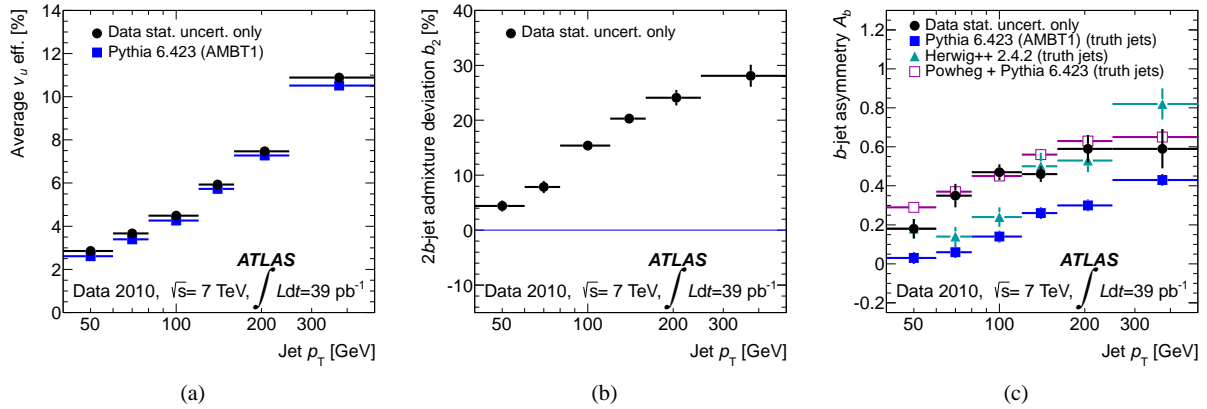asymmetry is corrected to the truth-particle jet level and compared with PYTHIA 6.423, Herwig++ 2.4.2 and POWHEG+PYTHIA 6.423 truth-particle jet predictions.

tions are different for dijet flavour fractions in the same p_T bin due to semileptonic decays of heavy flavour hadrons and different jet energy distributions for light and heavy flavour subleading jets.

The truth-particle dijet flavour fractions in each analysis bin are calculated using the following formula:

$$f_i^{\text{unfold}} = \frac{f_i/\varepsilon_i}{\sum_k (f_k/\varepsilon_k)}, \tag{18}$$

where f_i is a flavour fraction obtained in the fit and ε_i is the corresponding unfolding correction factor. The f_i^{unfold} does not coincide with the f_i because all correction factors ε_i in a given analysis bin are different, as explained earlier. Usually ε_i is smaller than one; therefore the normalisation in Eq.(18) is needed. The unfolded flavour fractions for truth-particle dijet events defined in Sect. 5 are presented in Table 2, as well as in Fig. 10, for the different leading jet p_T bins.

8.3 Systematic uncertainties

The measured dijet flavour fractions are subject to systematic uncertainties, due to the assumptions made in selecting the model parameters in Eq.(17) and the following effects:

– Reconstructed jets in data and Monte Carlo simulation may have different kinematic properties due to trigger requirements, jet energy scale (JES) uncertainties, cleaning cuts in the data selection procedure and event pile-up.
– Differences between data and Monte Carlo simulation in the template shapes are possible, despite the tuning of the template shape to the track resolution, and the adjustment of the fit to increase the fraction of jets with two b-quarks.

– The JES uncertainty and differences in energy between light and heavy flavour jets influence the unfolding correction factors. The template shapes are also affected by the remaining p_T dependence of the $B^\top$ variable.
– Imperfect description of bottom and charm hadron decay properties in Monte Carlo generators.

The influence of the differences in the jet p_T and rapidity distributions between data and Monte Carlo simulation on the analysis results is estimated by using PYTHIA 6.423 templates obtained with and without the p_T and rapidity reweighting, respectively. The differences in the results are taken as systematic uncertainties. Both make only minor contributions to the full systematic uncertainties. The influence of pile-up is estimated by adding minimum bias events to the PYTHIA 6.423 dijet events and repeating the analysis procedure. The effect is found to be negligible.

A potential bias due to the incorrect modelling of the JES is estimated by varying the jet energy response by its uncertainty [16]. Detailed studies have shown that the JES uncertainty is smallest in the central calorimeter region ($|\eta| < 0.8$) for jets with $p_T > 60$ GeV, with values of $\sim 2.5\%$, and that it is well below the 5% level for the whole kinematic range of this analysis. Both jets in a jet pair are varied simultaneously. An additional b-jet energy uncertainty is taken into account, and also applied for charm jets. Templates obtained from PYTHIA 6.423 events with modified jet energies are used for the data fit. Due to the dependence of the parameterisation of the charm and bottom vertex reconstruction efficiencies on jet p_T, these values are modified following the jet energy scaling. The systematic uncertainty due to the JES is estimated to be half of the difference between the fit results with positive and negative variation of the jet energy. The JES uncertainty is one of the major systematic uncertainties for all flavour fractions. In

Lead. jet p_T [GeV]	40–60	60–80	80–120	120–160	160–250	250–500
f_{BB} [%]	0.65±0.04±0.12	0.63±0.04±0.11	0.58±0.02±0.11	0.61±0.03±0.10	0.58±0.05±0.07	0.39±0.08±0.06
f_{BC} [%]	0.49±0.15±0.18	0.31±0.13±0.18	0.53±0.08±0.19	0.52±0.09±0.22	0.28±0.17±0.24	0.93±0.36±0.24
f_{CC} [%]	1.08±0.30±0.31	1.51±0.29±0.33	1.03±0.11±0.28	0.86±0.13±0.24	1.68±0.30±0.44	0.70±0.47±0.50
f_{BU} [%]	4.07±0.14±0.45	4.78±0.14±0.46	5.43±0.08±0.54	6.02±0.09±0.52	6.55±0.17±0.42	6.69±0.29±0.52
f_{CU} [%]	10.6±0.5±1.7	10.3±0.5±1.3	11.3±0.25±1.5	10.9±0.24±1.8	11.0±0.5±2.0	12.4±0.8±2.8
f_{UU} [%]	83.1±0.6±2.0	82.4±0.5±1.7	81.2±0.3±1.8	81.1±0.3±2.0	80.0±0.6±2.4	78.9±0.9±3.6

Table 2 The unfolded dijet flavour compositions for each leading jet p_T bin, with statistical uncertainties as first entries and the full systematic uncertainties as second entries.

particular, for f_{BU} and f_{CU} it varies from absolute values of 0.2 % and 1.1 % in the lowest p_T bin, to 0.1 % and 0.8 % in the highest p_T bin.

The charm and bottom secondary vertex reconstruction efficiencies are fixed in the analysis to the predictions for PYTHIA 6.423 dijet events, as explained in Sect. 7. To estimate possible deviations of these efficiencies, several Monte Carlo generators are used. The influences of a different proton structure function set (PYTHIA+CTEQ 6.6), a different parton fragmentation function (PYTHIA+Peterson), a different showering model (Herwig++), different charm and bottom hadron decays description (PYTHIA+EVTGEN) and additional track impact parameter smearing have been studied. Herwig++ shows the largest deviations in the secondary vertex reconstruction efficiency for bottom from the PYTHIA 6.423 Monte Carlo. The absolute difference is $\sim$ 6 % in the lowest p_T region, but decreases to $\sim$ 2 % in the highest p_T region. In the case of charm, PYTHIA+EVTGEN predicts the largest absolute deviations of $\sim$ 2 % from PYTHIA 6.423. Since the largest uncertainty in the vertex reconstruction efficiency comes from the fragmentation model (Herwig++) for bottom and from the charm hadron decay description (EVTGEN) for charm, the deviations in the charm and bottom vertex efficiencies are treated as independent for the systematic study. The systematic uncertainties in the flavour fractions are estimated by varying the charm and bottom vertex reconstruction efficiencies in the data fit by their maximal deviations. The uncertainty due to the bottom vertex efficiency is comparable with the JES uncertainty for the flavour fractions with bottom, and small otherwise. Similarly, the systematic uncertainty driven by the charm vertex efficiency is important for the fractions with charm.

The influence of imperfections in the Monte Carlo template shapes is estimated in two ways. The baseline templates are constructed from Monte Carlo jets passing the dijet selection procedure. Alternatively, one can use jets without a dijet selection. The templates obtained in this way are biased, due to different kinematic properties of the jets and changes in the contributions of the different heavy flavour production mechanisms. The number of contributing jets is also significantly larger, which makes these templates virtually independent from the baseline ones. To extract the sys-

tematic uncertainty, the data fit is redone with the inclusive jet templates. The statistical fluctuations due to the independent templates are reduced by smoothing the differences in the fit results, using a linear function fit over the whole analysis p_T range with weights $\sqrt{N_i}$, where N_i is the number of selected data events in bin i. The smoothed differences in the flavour fractions between data fits are taken as systematic uncertainties. In absolute values, they vary from 0.08 % in the lowest p_T bin to 0.2 % in the highest p_T bin for the f_{CC} fractions and from 0.06 % to 1.3 % for the f_{CU} fractions. This systematic uncertainty is significantly smaller for the other flavour fractions.

Another check of the influence of the template shape is made by generating templates using Herwig++ instead of PYTHIA 6.423. The dedicated simulation model described in Sect. 7.3 is exploited for this study. The PYTHIA 6.423 fully simulated vertices are used for template creation, but pseudo-data are created with Herwig++ vertices. Then the standard analysis procedure is applied. The averaged values based on 200 pseudo-experiments are compared with the initial fast simulation model parameters and the differences are considered as systematic uncertainties. Overall, the systematic uncertainty due to the template shapes constitutes a large contribution to the full systematic uncertainty for all flavour fractions, and is similar in size to those from JES and secondary vertex reconstruction efficiencies.

The predictions of the Monte Carlo simulation for the amount of heavy flavour in the leading and subleading jets differ significantly from one generator to another, as can be seen in Fig. 3. In the current analysis the charm production asymmetry is fixed to the PYTHIA 6.423 prediction. To determine the systematic effect of an imprecise description of the charm asymmetry, the data fit is redone with the charm asymmetry values given by POWHEG+PYTHIA 6.423 as shown in Fig. 3. This systematic uncertainty reaches ~ 40 % of the total uncertainty for the f_{CC} fraction and ~ 20 % for the f_{BC} fraction in the high p_T region, in all other cases it is below ~ 10 %. The admixture of jets with two charm quarks inside is also fixed to the PYTHIA 6.423 prediction in the analysis. To determine the systematic effect due to this, the double-charm admixture is varied by a fixed value, equal to 1/3 of the measured double-bottom jet admixture. This

choice is justified by a comparison of the bottom and charm asymmetries in Fig. 3, which are governed by similar QCD effects. This systematic uncertainty becomes important for the f_{CU} and f_{BU} fractions for large p_T. In absolute values, it is 1.2 % for f_{CU} and 0.35 % for f_{BU} in the $[250, 500]$ GeV bin.

To improve the agreement between data and Monte Carlo simulation, the flavour template shapes are tuned on the 2010 data as described in Sect. 6.4. The systematic uncertainties due to this procedure are estimated by repeating the full analysis using the fully smeared ($F_{smear} = 1.0$, see Sect. 6.4) PYTHIA 6.423 dijet sample for template construction and definition of the vertex reconstruction efficiencies. This systematic uncertainty is ~ 50 % of the total systematic uncertainty for the f_{BU} fraction in the high p_T region and significantly smaller in other cases.

The unfolding procedure for obtaining the dijet flavour fractions at the truth-particle level is based on estimations of the dijet reconstruction efficiencies from Monte Carlo simulation. Systematic uncertainties on these are estimated using the differences in the unfolded flavour fractions calculated with the unfolding coefficients predicted by PYTHIA 6.423 and Herwig++ 2.4.2. The flavour dijet reconstruction efficiencies are calculated for each analysis p_T bin and therefore also depend on the JES modelling. The changes in the unfolded flavour fractions due to the shifted jet energies are considered as the JES-induced unfolding systematic uncertainties. In both cases, the differences in the unfolded flavour fractions have significant statistical fluctuations due to the fact that the number of Monte Carlo events used for the reconstruction efficiency estimation is limited. The differences for each flavour fraction are therefore smoothed in the same way as the template shape systematic uncertainty. In the low p_T bins the systematic uncertainties due to the unfolding are comparable in size to the uncertainties from JES and template shapes for f_{CC}, f_{BU} and f_{CU}. In all other cases they are relatively small.

The full systematic uncertainties on the unfolded dijet flavour fractions are presented in Table 2. These uncertainties are added in quadrature to the statistical uncertainties and are shown as shaded bands in Fig. 10. Except for BU, all data fractions are in agreement within the uncertainties with the predictions of the LO and NLO generators. The BU fraction, while coinciding reasonably well with the Monte Carlo simulation predictions at low jet p_T, shows disagreement for jets with p_T above ~ 100 GeV. The discrepancy of the BU data points with the PYTHIA 6.423 prediction in the four high p_T analysis bins has a significance of 4.3 standard deviations, corresponding to a fluctuation probability of 8.7×10^{-6}.

9 Conclusions

An analysis of the flavour composition of dijet events has been performed, based on an integrated luminosity of 39 pb^{-1} collected by the ATLAS detector in 2010 at a centre-of-mass energy of 7 TeV. The analysis makes use of reconstructed secondary vertices in jets, without explicitly assigning individual flavours. Instead, kinematic properties of the ensemble of tracks associated with a secondary vertex are used to distinguish between light, charm and bottom jets. Specially constructed and optimised variables that are highly sensitive to the flavour content of jets, have been employed. The dijet heavy flavour fractions are determined from a multidimensional fit using templates of these variables.

The analysis demonstrates the capability of ATLAS to measure the dijet fractions containing bottom jets and the more challenging charm jets down to the level of ~ 0.5 %. All five dijet final states with heavy flavours are reliably extracted and measured as a function of the leading jet p_T.

A significant difference in the bottom hadron content between leading and subleading jets is observed. This difference is poorly described by the LO generators PYTHIA 6.423 and Herwig++ 2.4.2, whereas the NLO generator POWHEG reproduces the data well.

The data-driven b-jet shape approach used in the fit demonstrates a deficiency of the b-jet template obtained with PYTHIA 6.423, particularly in the high jet p_T region. An increase of the template contribution describing the presence of two b-hadrons inside a jet substantially improves the agreement between data and Monte Carlo simulation.

The measurements of the six dijet flavour fractions are compared with the predictions of the two LO generators PYTHIA 6.423 and Herwig++ 2.4.2, and also with the NLO generator POWHEG. All generator predictions are consistent with each other and agree with the measured values, except for the mixed BU dijet fraction, which is systematically above all the predictions in the high p_T region.

10 Acknowledgements
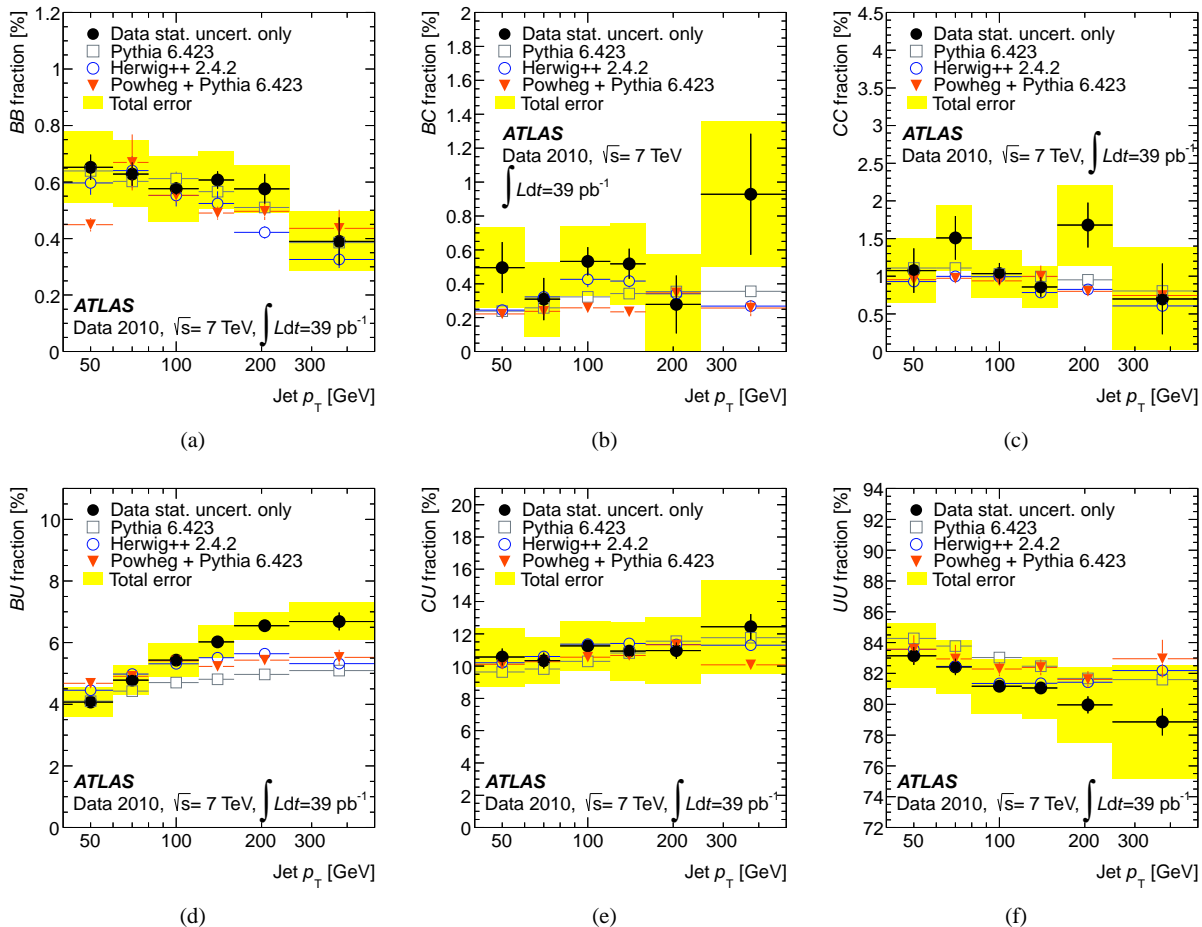
Fig. 10 The unfolded dijet flavour fractions for each leading jet p_T bin (black points) with PYTHIA 6.423 (squares), Herwig++ 2.4.2 (circles) and POWHEG+PYTHIA 6.423 (filled triangles) predictions overlaid. The error bars on the data points show statistical uncertainties only, whereas the full uncertainties appear as shaded bands.

References

1. D0 Collaboration, B. Abbott, et al., The $b\bar{b}$ Production Section and Angular Correlations in $p\bar{p}$ Collisions at $\sqrt{s}$ = 1.8 TeV, Phys. Lett. B **487**, 264 (2000)
2. D0 Collaboration, B. Abbott, et al., Cross Section for b Jet Production in $p\bar{p}$ Collisions at $\sqrt{s}$ = 1.8 TeV, Phys. Rev. Lett. **85**, 5068 (2000)
3. CDF Collaboration, T. Aaltonen, et al., Measurement of Correlated $b\bar{b}$ Production in $p\bar{p}$ Collisions at $\sqrt{s}$ = 1960 GeV, Phys. Rev. D **77**, 072004 (2008)
4. S. Seidel, Heavy Quark Production at the Tevatron, arXiv:0808.3347 [hep-ex], (2008)
5. I. Kenyon, The Measurement of the Cross Section for Beauty Production at the CERN Anti-p p Collider, J. Phys. G **15**, 1087 (1989)
6. C. Lourenco, H. Wohri, Heavy Flavour Hadroproduction from Fixed-Target to Collider Energies, Phys. Rept. **433**, 127 (2006)
7. CMS Collaboration, Inclusive b-Jet Production in pp Collisions at $\sqrt{s}$ = 7 TeV, J. High Energy Phys. **1204**, 084 (2012)

8. CMS Collaboration, Measurement of the Cross Section for Production of $b\bar{b}X$ Decaying to Muons in pp Collisions at $\sqrt{s} =$ 7 TeV, J. High Energy Phys. **1206**, 110 (2012)

9. CMS Collaboration, Inclusive b-Hadron Production Cross Section with Muons in pp Collisions at $\sqrt{s} =$ 7 TeV, J. High Energy Phys. **1103**, 090 (2011)

10. CMS Collaboration, Measurement of $B\bar{B}$ Angular Correlations Based on Secondary Vertex Reconstruction at $\sqrt{s} =$ 7 TeV, J. High Energy Phys. **1103**, 136 (2011)

11. LHCb Collaboration, Measurement of $\sigma(pp \rightarrow b\bar{b}X)$ at $\sqrt{s} =$ 7 TeV in the Forward Region, Phys. Lett.B **694**, 209 (2010)

12. ATLAS Collaboration, Measurement of the Inclusive and Dijet Cross Sections of b-Jets in pp Collisions at $\sqrt{s} =$ 7 TeV with the ATLAS Detector, Eur. Phys. J. C **71**, 1846 (2011)

13. ATLAS Collaboration, The ATLAS experiment at the CERN Large Hadron Collider, JINST **3**, S08003 (2008)

14. M. Cacciari, G.P. Salam, G. Soyez, The Anti-k_t Jet Clustering Algorithm, J. High Energy Phys. **0804**, 063 (2008)

15. ATLAS Collaboration, Data-Quality Requirements and Event Cleaning for Jets and Missing Transverse Energy Reconstruction with the ATLAS Detector in Proton-Proton Collisions at a Center-of-Mass Energy of $\sqrt{s} =$ 7 TeV, ATLAS-CONF-2010-038

16. ATLAS Collaboration, Jet Energy Measurement with the ATLAS Detector in Proton-Proton Collisions at $\sqrt{s} =$ 7 TeV, arXiv:1112.6426 [hep-ex], submitted to Eur. Phys. J. C

17. ATLAS Collaboration, Expected Performance of the ATLAS Experiment - Detector, Trigger and Physics, arXiv:0901.0512 [hep-ph], (2009)

18. T. Sjostrand, S. Mrenna, P.Z. Skands, PYTHIA 6.4 Physics and Manual, J. High Energy Phys. **0605**, 026 (2006)

19. A. Sherstnev, R. Thorne, Parton Distributions for LO Generators, Eur. Phys. J. C **55**, 553 (2008)

20. ATLAS, Charged Particle Multiplicities in pp Interactions at $\sqrt{s} =$ 0.9 TeV and 7 TeV in a Difractive Limited Phase-Space Measured with the ATLAS Detector at the LHC and New PYTHIA 6 Tune, ATLAS-CONF-2010-031

21. M. Bahr, S. Gieseke, M. Gigg, D. Grellscheid, K. Hamilton, et al., Herwig++ 2.3 Release Note, (2008)

22. P.M. Nadolsky, H.L. Lai, Q.H. Cao, J. Huston, J. Pumplin, et al., Implications of CTEQ Global Analysis for Collider Observables, Phys. Rev. D **78**, 013004 (2008)

23. G. Corcella, I. Knowles, G. Marchesini, S. Moretti, K. Odagiri, et al., Herwig 6: An Event Generator for Hadron Emission Reactions with Interfering Gluons (Including Supersymmetric Processes), J. High Energy Phys. **0101**, 010 (2001)

24. J. Butterworth, J.R. Forshaw, M. Seymour, Multiparton Interactions in Photoproduction at HERA, Z. Phys. C **72**, 637 (1996)

25. J. Butterworth, M. Seymour. JIMMY 4: Multiparton Interactions in Herwig for the LHC. http://projects.hepforge.org/jimmy/ (2004)

26. ATLAS Collaboration, First Tuning of Herwig/JIMMY to ATLAS Data, Tech. Rep. ATL-PHYS-PUB-2010-014, CERN, Geneva (2010)

27. D. Lange, The EvtGen Particle Decay Simulation Package, Nucl. Instrum. Methods A **462**, 152 (2001)

28. S. Alioli, P. Nason, C. Oleari, E. Re, A General Framework for Implementing NLO Calculations in Shower Monte Carlo Programs: the POWHEG BOX, J. High Energy Phys. **1006**, 043 (2010)

29. P. Nason, A New Method for Combining NLO QCD with Shower Monte Carlo Algorithms, J. High Energy Phys. **0411**, 040 (2004)

30. S. Frixione, P. Nason, C. Oleari, Matching NLO QCD Computations with Parton Shower Simulations: the POWHEG Method, J. High Energy Phys. **0711**, 070 (2007)

31. S. Alioli, K. Hamilton, P. Nason, C. Oleari, E. Re, Jet Pair Production in POWHEG, J. High Energy Phys. **1104**, 081 (2011)

32. A. Martin, W. Stirling, R. Thorne, G. Watt, Parton Distributions for the LHC, Eur. Phys. J. C **63**, 189 (2009)

33. ATLAS Collaboration, The ATLAS Simulation Infrastructure, Eur. Phys. J. C **70**, 823 (2010)

34. GEANT4, S. Agostinelli, et al., GEANT 4: A Simulation Toolkit, Nucl. Instrum. Methods A **506**, 250 (2003)

35. E. Norrbin, T. Sjostrand, Production and Hadronization of Heavy Quarks, Eur. Phys. J. C **17**, 137 (2000)

36. Particle Data Group, K. Nakamura, et al., Review of Particle Physics, J. Phys. G **37**, 075021 (2010)

37. CDF Collaboration, T. Aaltonen, et al., Measurement of b-Jet Shapes in Inclusive Jet Production in $p\bar{p}$ Collisions at $\sqrt{s} =$ 1.96 TeV, Phys. Rev. D **78**, 072005 (2008)

38. ATLAS Collaboration, Tracking Studies for b-tagging with 7 TeV Collision Data with the ATLAS Detector, ATLAS-CONF-2010-070

39. F. James, M. Roos, Minuit: A System for Function Minimization and Analysis of the Parameter Errors and Correlations, Comput. Phys. Commun. **10**, 343 (1975)

40. R. Brun, F. Rademakers, ROOT: An Object Oriented Data Analysis Framework, Nucl. Instrum. Methods A **389**(12), 81 (1997)

The ATLAS Collaboration

G. Aad[48], T. Abajyan[21], B. Abbott[111], J. Abdallah[12], S. Abdel Khalek[115], A.A. Abdelalim[49], O. Abdinov[11], R. Aben[105], B. Abi[112], M. Abolins[88], O.S. AbouZeid[158], H. Abramowicz[153], H. Abreu[136], E. Acerbi[89a,89b], B.S. Acharya[164a,164b], L. Adamczyk[38], D.L. Adams[25], T.N. Addy[56], J. Adelman[176], S. Adomeit[98], P. Adragna[75], T. Adye[129], S. Aefsky[23], J.A. Aguilar-Saavedra[124b,a], M. Agustoni[17], M. Aharrouche[81], S.P. Ahlen[22], F. Ahles[48], A. Ahmad[148], M. Ahsan[41], G. Aielli[133a,133b], T. Akdogan[19a], T.P.A. Åkesson[79], G. Akimoto[155], A.V. Akimov[94], M.S. Alam[2], M.A. Alam[76], J. Albert[169], S. Albrand[55], M. Aleksa[30], I.N. Aleksandrov[64], F. Alessandria[89a], C. Alexa[26a], G. Alexander[153], G. Alexandre[49], T. Alexopoulos[10], M. Alhroob[164a,164c], M. Aliev[16], G. Alimonti[89a], J. Alison[120], B.M.M. Allbrooke[18], P.P. Allport[73], S.E. Allwood-Spiers[53], J. Almond[82], A. Aloisio[102a,102b], R. Alon[172], A. Alonso[79], F. Alonso[70], B. Alvarez Gonzalez[88], M.G. Alviggi[102a,102b], K. Amako[65], C. Amelung[23], V.V. Ammosov[128,*], S.P. Amor Dos Santos[124a], A. Amorim[124a,b], N. Amram[153], C. Anastopoulos[30], L.S. Ancu[17], N. Andari[115], T. Andeen[35], C.F. Anders[58b], G. Anders[58a], K.J. Anderson[31], A. Andreazza[89a,89b], V. Andrei[58a], M-L. Andrieux[55], X.S. Anduaga[70], P. Anger[44], A. Angerami[35], F. Anghinolfi[30], A. Anisenkov[107], N. Anjos[124a], A. Annovi[47], A. Antonaki[9], M. Antonelli[47], A. Antonov[96], J. Antos[144b], F. Anulli[132a], M. Aoki[101], S. Aoun[83], L. Aperio Bella[5], R. Apolle[118,c], G. Arabidze[88], I. Aracena[143], Y. Arai[65], A.T.H. Arce[45], S. Arfaoui[148], J-F. Arguin[15], E. Arik[19a,*], M. Arik[19a], A.J. Armbruster[87], O. Arnaez[81], V. Arnal[80], C. Arnault[115], A. Artamonov[95], G. Artoni[132a,132b], D. Arutinov[21], S. Asai[155], R. Asfandiyarov[173], S. Ask[28], B. Åsman[146a,146b], L. Asquith[6], K. Assamagan[25], A. Astbury[169], M. Atkinson[165], B. Aubert[5], E. Auge[115], K. Augsten[127], M. Aurousseau[145a], G. Avolio[163], R. Avramidou[10], D. Axen[168], G. Azuelos[93,d], Y. Azuma[155], M.A. Baak[30], G. Baccaglioni[89a], C. Bacci[134a,134b], A.M. Bach[15], H. Bachacou[136], K. Bachas[30], M. Backes[49], M. Backhaus[21], E. Badescu[26a], P. Bagnaia[132a,132b], S. Bahinipati[3], Y. Bai[33a], D.C. Bailey[158], T. Bain[158], J.T. Baines[129], O.K. Baker[176], M.D. Baker[25], S. Baker[77], E. Banas[39], P. Banerjee[93], Sw. Banerjee[173], D. Banfi[30], A. Bangert[150], V. Bansal[169], H.S. Bansil[18], L. Barak[172], S.P. Baranov[94], A. Barbaro Galtieri[15], T. Barber[48], E.L. Barberio[86], D. Barberis[50a,50b], M. Barbero[21], D.Y. Bardin[64], T. Barillari[99], M. Barisonzi[175], T. Barklow[143], N. Barlow[28], B.M. Barnett[129], R.M. Barnett[15], A. Baroncelli[134a], G. Barone[49], A.J. Barr[118], F. Barreiro[80], J. Barreiro Guimarães da Costa[57], P. Barrillon[115], R. Bartoldus[143], A.E. Barton[71], V. Bartsch[149], A. Basye[165], R.L. Bates[53], L. Batkova[144a], J.R. Batley[28], A. Battaglia[17], M. Battistin[30], F. Bauer[136], H.S. Bawa[143,e], S. Beale[98], T. Beau[78], P.H. Beauchemin[161], R. Beccherle[50a], P. Bechtle[21], H.P. Beck[17], A.K. Becker[175], S. Becker[98], M. Beckingham[138], K.H. Becks[175], A.J. Beddall[19c], A. Beddall[19c], S. Bedikian[176], V.A. Bednyakov[64], C.P. Bee[83], L.J. Beemster[105], M. Begel[25], S. Behar Harpaz[152], P.K. Behera[62], M. Beimforde[99], C. Belanger-Champagne[85], P.J. Bell[49], W.H. Bell[49], G. Bella[153], L. Bellagamba[20a], F. Bellina[30], M. Bellomo[30], A. Belloni[57], O. Beloborodova[107,f], K. Belotskiy[96], O. Beltramello[30], O. Benary[153], D. Benchekroun[135a], K. Bendtz[146a,146b], N. Benekos[165], Y. Benhammou[153], E. Benhar Noccioli[49], J.A. Benitez Garcia[159b], D.P. Benjamin[45], M. Benoit[115], J.R. Bensinger[23], K. Benslama[130], S. Bentvelsen[105], D. Berge[30], E. Bergeaas Kuutmann[42], N. Berger[5], F. Berghaus[169], E. Berglund[105], J. Beringer[15], P. Bernat[77], R. Bernhard[48], C. Bernius[25], T. Berry[76], C. Bertella[83], A. Bertin[20a,20b], F. Bertolucci[122a,122b], M.I. Besana[89a,89b], G.J. Besjes[104], N. Besson[136], S. Bethke[99], W. Bhimji[46], R.M. Bianchi[30], M. Bianco[72a,72b], O. Biebel[98], S.P. Bieniek[77], K. Bierwagen[54], J. Biesiada[15], M. Biglietti[134a], H. Bilokon[47], M. Bindi[20a,20b], S. Binet[115], A. Bingul[19c], C. Bini[132a,132b], C. Biscarat[178], B. Bittner[99], K.M. Black[22], R.E. Blair[6], J.-B. Blanchard[136], G. Blanchot[30], T. Blazek[144a], I. Bloch[42], C. Blocker[23], J. Blocki[39], A. Blondel[49], W. Blum[81], U. Blumenschein[54], G.J. Bobbink[105], V.B. Bobrovnikov[107], S.S. Bocchetta[79], A. Bocci[45], C.R. Boddy[118], M. Boehler[48], J. Boek[175], N. Boelaert[36], J.A. Bogaerts[30], A. Bogdanchikov[107], A. Bogouch[90,*], C. Bohm[146a], J. Bohm[125], V. Boisvert[76], T. Bold[38], V. Boldea[26a], N.M. Bolnet[136], M. Bomben[78], M. Bona[75], M. Boonekamp[136], C.N. Booth[139], S. Bordoni[78], C. Borer[17], A. Borisov[128], G. Borissov[71], I. Borjanovic[13a], M. Borri[82], S. Borroni[87], V. Bortolotto[134a,134b], K. Bos[105], D. Boscherini[20a], M. Bosman[12], H. Boterenbrood[105], J. Bouchami[93], J. Boudreau[123], E.V. Bouhova-Thacker[71], D. Boumediene[34], C. Bourdarios[115], N. Bousson[83], A. Boveia[31], J. Boyd[30], I.R. Boyko[64], I. Bozovic-Jelisavcic[13b], J. Bracinik[18], P. Branchini[134a], G.W. Brandenburg[57], A. Brandt[8], G. Brandt[118], O. Brandt[54], U. Bratzler[156], B. Brau[84], J.E. Brau[114], H.M. Braun[175,*], S.F. Brazzale[164a,164c], B. Brelier[158], J. Bremer[30], K. Brendlinger[120], R. Brenner[166], S. Bressler[172], D. Britton[53], F.M. Brochu[28], I. Brock[21], R. Brock[88], F. Broggi[89a], C. Bromberg[88], J. Bronner[99], G. Brooijmans[35], T. Brooks[76], W.K. Brooks[32b], G. Brown[82], H. Brown[8], P.A. Bruckman de Renstrom[39], D. Bruncko[144b], R. Bruneliere[48], S. Brunet[60], A. Bruni[20a], G. Bruni[20a], M. Bruschi[20a], T. Buanes[14], Q. Buat[55], F. Bucci[49], J. Buchanan[118], P. Buchholz[141], R.M. Buckingham[118], A.G. Buckley[46], S.I. Buda[26a], I.A. Budagov[64], B. Budick[108], V. Büscher[81], L. Bugge[117], O. Bulekov[96], A.C. Bundock[73], M. Bunse[43], T. Buran[117], H. Burckhart[30], S. Burdin[73], T. Burgess[14], S. Burke[129], E. Busato[34], P. Bussey[53], C.P. Buszello[166], B. Butler[143], J.M. Butler[22], C.M. Buttar[53], J.M. Butterworth[77], W. Buttinger[28], M. Byszewski[30], S. Cabrera Urbán[167], D. Caforio[20a,20b], O. Cakir[4a], P. Calafiura[15], G. Calderini[78],

P. Calfayan[98], R. Calkins[106], L.P. Caloba[24a], R. Caloi[132a,132b], D. Calvet[34], S. Calvet[34], R. Camacho Toro[34],
P. Camarri[133a,133b], D. Cameron[117], L.M. Caminada[15], R. Caminal Armadans[12], S. Campana[30], M. Campanelli[77],
V. Canale[102a,102b], F. Canelli[31,g], A. Canepa[159a], J. Cantero[80], R. Cantrill[76], L. Capasso[102a,102b],
M.D.M. Capeans Garrido[30], I. Caprini[26a], M. Caprini[26a], D. Capriotti[99], M. Capua[37a,37b], R. Caputo[81], R. Cardarelli[133a],
T. Carli[30], G. Carlino[102a], L. Carminati[89a,89b], B. Caron[85], S. Caron[104], E. Carquin[32b], G.D. Carrillo-Montoya[173],
A.A. Carter[75], J.R. Carter[28], J. Carvalho[124a,h], D. Casadei[108], M.P. Casado[12], M. Cascella[122a,122b], C. Caso[50a,50b,*],
A.M. Castaneda Hernandez[173,i], E. Castaneda-Miranda[173], V. Castillo Gimenez[167], N.F. Castro[124a], G. Cataldi[72a],
P. Catastini[57], A. Catinaccio[30], J.R. Catmore[30], A. Cattai[30], G. Cattani[133a,133b], S. Caughron[88], V. Cavaliere[165],
P. Cavalleri[78], D. Cavalli[89a], M. Cavalli-Sforza[12], V. Cavasinni[122a,122b], F. Ceradini[134a,134b], A.S. Cerqueira[24b], A. Cerri[30],
L. Cerrito[75], F. Cerutti[47], S.A. Cetin[19b], A. Chafaq[135a], D. Chakraborty[106], I. Chalupkova[126], K. Chan[3], P. Chang[165],
B. Chapleau[85], J.D. Chapman[28], J.W. Chapman[87], E. Chareyre[78], D.G. Charlton[18], V. Chavda[82], C.A. Chavez Barajas[30],
S. Cheatham[85], S. Chekanov[6], S.V. Chekulaev[159a], G.A. Chelkov[64], M.A. Chelstowska[104], C. Chen[63], H. Chen[25],
S. Chen[33c], X. Chen[173], Y. Chen[35], A. Cheplakov[64], R. Cherkaoui El Moursli[135e], V. Chernyatin[25], E. Cheu[7],
S.L. Cheung[158], L. Chevalier[136], G. Chiefari[102a,102b], L. Chikovani[51a,*], J.T. Childers[30], A. Chilingarov[71], G. Chiodini[72a],
A.S. Chisholm[18], R.T. Chislett[77], A. Chitan[26a], M.V. Chizhov[64], G. Choudalakis[31], S. Chouridou[137], I.A. Christidi[77],
A. Christov[48], D. Chromek-Burckhart[30], M.L. Chu[151], J. Chudoba[125], G. Ciapetti[132a,132b], A.K. Ciftci[4a], R. Ciftci[4a],
D. Cinca[34], V. Cindro[74], C. Ciocca[20a,20b], A. Ciocio[15], M. Cirilli[87], P. Cirkovic[13b], Z.H. Citron[172], M. Citterio[89a],
M. Ciubancan[26a], A. Clark[49], P.J. Clark[46], R.N. Clarke[15], W. Cleland[123], J.C. Clemens[83], B. Clement[55],
C. Clement[146a,146b], Y. Coadou[83], M. Cobal[164a,164c], A. Coccaro[138], J. Cochran[63], J.G. Cogan[143], J. Coggeshall[165],
E. Cogneras[178], J. Colas[5], S. Cole[106], A.P. Colijn[105], N.J. Collins[18], C. Collins-Tooth[53], J. Collot[55], T. Colombo[119a,119b],
G. Colon[84], P. Conde Muiño[124a], E. Coniavitis[118], M.C. Conidi[12], S.M. Consonni[89a,89b], V. Consorti[48],
S. Constantinescu[26a], C. Conta[119a,119b], G. Conti[57], F. Conventi[102a,j], M. Cooke[15], B.D. Cooper[77], A.M. Cooper-Sarkar[118],
K. Copic[15], T. Cornelissen[175], M. Corradi[20a], F. Corriveau[85,k], A. Cortes-Gonzalez[165], G. Cortiana[99], G. Costa[89a],
M.J. Costa[167], D. Costanzo[139], D. Côté[30], L. Courneyea[169], G. Cowan[76], C. Cowden[28], B.E. Cox[82], K. Cranmer[108],
F. Crescioli[122a,122b], M. Cristinziani[21], G. Crosetti[37a,37b], S. Crépé-Renaudin[55], C.-M. Cuciuc[26a], C. Cuenca Almenar[176],
T. Cuhadar Donszelmann[139], M. Curatolo[47], C.J. Curtis[18], C. Cuthbert[150], P. Cwetanski[60], H. Czirr[141], P. Czodrowski[44],
Z. Czyczula[176], S. D'Auria[53], M. D'Onofrio[73], A. D'Orazio[132a,132b], M.J. Da Cunha Sargedas De Sousa[124a], C. Da Via[82],
W. Dabrowski[38], A. Dafinca[118], T. Dai[87], C. Dallapiccola[84], M. Dam[36], M. Dameri[50a,50b], D.S. Damiani[137],
H.O. Danielsson[30], V. Dao[49], G. Darbo[50a], G.L. Darlea[26b], J.A. Dassoulas[42], W. Davey[21], T. Davidek[126], N. Davidson[86],
R. Davidson[71], E. Davies[118,c], M. Davies[93], O. Davignon[78], A.R. Davison[77], Y. Davygora[58a], E. Dawe[142], I. Dawson[139],
R.K. Daya-Ishmukhametova[23], K. De[8], R. de Asmundis[102a], S. De Castro[20a,20b], S. De Cecco[78], J. de Graat[98],
N. De Groot[104], P. de Jong[105], C. De La Taille[115], H. De la Torre[80], F. De Lorenzi[63], L. de Mora[71], L. De Nooij[105],
D. De Pedis[132a], A. De Salvo[132a], U. De Sanctis[164a,164c], A. De Santo[149], J.B. De Vivie De Regie[115], G. De Zorzi[132a,132b],
W.J. Dearnaley[71], R. Debbe[25], C. Debenedetti[46], B. Dechenaux[55], D.V. Dedovich[64], J. Degenhardt[120], C. Del Papa[164a,164c],
J. Del Peso[80], T. Del Prete[122a,122b], T. Delemontex[55], M. Deliyergiyev[74], A. Dell'Acqua[30], L. Dell'Asta[22],
M. Della Pietra[102a,j], D. della Volpe[102a,102b], M. Delmastro[5], P.A. Delsart[55], C. Deluca[105], S. Demers[176], M. Demichev[64],
B. Demirkoz[12,l], J. Deng[163], S.P. Denisov[128], D. Derendarz[39], J.E. Derkaoui[135d], F. Derue[78], P. Dervan[73], K. Desch[21],
E. Devetak[148], P.O. Deviveiros[105], A. Dewhurst[129], B. DeWilde[148], S. Dhaliwal[158], R. Dhullipudi[25,m],
A. Di Ciaccio[133a,133b], L. Di Ciaccio[5], A. Di Girolamo[30], B. Di Girolamo[30], S. Di Luise[134a,134b], A. Di Mattia[173],
B. Di Micco[30], R. Di Nardo[47], A. Di Simone[133a,133b], R. Di Sipio[20a,20b], M.A. Diaz[32a], E.B. Diehl[87], J. Dietrich[42],
T.A. Dietzsch[58a], S. Diglio[86], K. Dindar Yagci[40], J. Dingfelder[21], F. Dinut[26a], C. Dionisi[132a,132b], P. Dita[26a], S. Dita[26a],
F. Dittus[30], F. Djama[83], T. Djobava[51b], M.A.B. do Vale[24c], A. Do Valle Wemans[124a,n], T.K.O. Doan[5], M. Dobbs[85],
R. Dobinson[30,*], D. Dobos[30], E. Dobson[30,o], J. Dodd[35], C. Doglioni[49], T. Doherty[53], Y. Doi[65,*], J. Dolejsi[126], I. Dolenc[74],
Z. Dolezal[126], B.A. Dolgoshein[96,*], T. Dohmae[155], M. Donadelli[24d], J. Donini[34], J. Dopke[30], A. Doria[102a],
A. Dos Anjos[173], A. Dotti[122a,122b], M.T. Dova[70], A.D. Doxiadis[105], A.T. Doyle[53], N. Dressnandt[120], M. Dris[10],
J. Dubbert[99], S. Dube[15], E. Duchovni[172], G. Duckeck[98], D. Duda[175], A. Dudarev[30], F. Dudziak[63], M. Dührssen[30],
I.P. Duerdoth[82], L. Duflot[115], M-A. Dufour[85], L. Duguid[76], M. Dunford[30], H. Duran Yildiz[4a], R. Duxfield[139],
M. Dwuznik[38], F. Dydak[30], M. Düren[52], W.L. Ebenstein[45], J. Ebke[98], S. Eckweiler[81], K. Edmonds[81], W. Edson[2],
C.A. Edwards[76], N.C. Edwards[53], W. Ehrenfeld[42], T. Eifert[143], G. Eigen[14], K. Einsweiler[15], E. Eisenhandler[75],
T. Ekelof[166], M. El Kacimi[135c], M. Ellert[166], S. Elles[5], F. Ellinghaus[81], K. Ellis[75], N. Ellis[30], J. Elmsheuser[98], M. Elsing[30],
D. Emeliyanov[129], R. Engelmann[148], A. Engl[98], B. Epp[61], A. Eppard[54], A. Ereditato[17], D. Eriksson[146a], J. Ernst[2],
M. Ernst[25], J. Ernwein[136], D. Errede[165], S. Errede[165], E. Ertel[81], M. Escalier[115], H. Esch[43], C. Escobar[123],
X. Espinal Curull[12], B. Esposito[47], F. Etienne[83], A.I. Etienvre[136], E. Etzion[153], D. Evangelakou[54], H. Evans[60],

L. Fabbri[20a,20b], C. Fabre[30], R.M. Fakhrutdinov[128], S. Falciano[132a], Y. Fang[173], M. Fanti[89a,89b], A. Farbin[8], A. Farilla[134a],
J. Farley[148], T. Farooque[158], S. Farrell[163], S.M. Farrington[170], P. Farthouat[30], F. Fassi[167], P. Fassnacht[30], D. Fassouliotis[9],
B. Fatholahzadeh[158], A. Favareto[89a,89b], L. Fayard[115], S. Fazio[37a,37b], R. Febbraro[34], P. Federic[144a], O.L. Fedin[121],
W. Fedorko[88], M. Fehling-Kaschek[48], L. Feligioni[83], D. Fellmann[6], C. Feng[33d], E.J. Feng[6], A.B. Fenyuk[128],
J. Ferencei[144b], W. Fernando[6], S. Ferrag[53], J. Ferrando[53], V. Ferrara[42], A. Ferrari[166], P. Ferrari[105], R. Ferrari[119a],
D.E. Ferreira de Lima[53], A. Ferrer[167], D. Ferrere[49], C. Ferretti[87], A. Ferretto Parodi[50a,50b], M. Fiascaris[31], F. Fiedler[81],
A. Filipčič[74], F. Filthaut[104], M. Fincke-Keeler[169], M.C.N. Fiolhais[124a,h], L. Fiorini[167], A. Firan[40], G. Fischer[42],
M.J. Fisher[109], M. Flechl[48], I. Fleck[141], J. Fleckner[81], P. Fleischmann[174], S. Fleischmann[175], T. Flick[175], A. Floderus[79],
L.R. Flores Castillo[173], M.J. Flowerdew[99], T. Fonseca Martin[17], A. Formica[136], A. Forti[82], D. Fortin[159a], D. Fournier[115],
A.J. Fowler[45], H. Fox[71], P. Francavilla[12], M. Franchini[20a,20b], S. Franchino[119a,119b], D. Francis[30], T. Frank[172], S. Franz[30],
M. Fraternali[119a,119b], S. Fratina[120], S.T. French[28], C. Friedrich[42], F. Friedrich[44], R. Froeschl[30], D. Froidevaux[30],
J.A. Frost[28], C. Fukunaga[156], E. Fullana Torregrosa[30], B.G. Fulsom[143], J. Fuster[167], C. Gabaldon[30], O. Gabizon[172],
T. Gadfort[25], S. Gadomski[49], G. Gagliardi[50a,50b], P. Gagnon[60], C. Galea[98], B. Galhardo[124a], E.J. Gallas[118], V. Gallo[17],
B.J. Gallop[129], P. Gallus[125], K.K. Gan[109], Y.S. Gao[143,e], A. Gaponenko[15], F. Garberson[176], M. Garcia-Sciveres[15],
C. García[167], J.E. García Navarro[167], R.W. Gardner[31], N. Garelli[30], H. Garitaonandia[105], V. Garonne[30], C. Gatti[47],
G. Gaudio[119a], B. Gaur[141], L. Gauthier[136], P. Gauzzi[132a,132b], I.L. Gavrilenko[94], C. Gay[168], G. Gaycken[21], E.N. Gazis[10],
P. Ge[33d], Z. Gecse[168], C.N.P. Gee[129], D.A.A. Geerts[105], Ch. Geich-Gimbel[21], K. Gellerstedt[146a,146b], C. Gemme[50a],
A. Gemmell[53], M.H. Genest[55], S. Gentile[132a,132b], M. George[54], S. George[76], P. Gerlach[175], A. Gershon[153],
C. Geweniger[58a], H. Ghazlane[135b], N. Ghodbane[34], B. Giacobbe[20a], S. Giagu[132a,132b], V. Giakoumopoulou[9],
V. Giangiobbe[12], F. Gianotti[30], B. Gibbard[25], A. Gibson[158], S.M. Gibson[30], M. Gilchriese[15], D. Gillberg[29],
A.R. Gillman[129], D.M. Gingrich[3,d], J. Ginzburg[153], N. Giokaris[9], M.P. Giordani[164c], R. Giordano[102a,102b], F.M. Giorgi[16],
P. Giovannini[99], P.F. Giraud[136], D. Giugni[89a], M. Giunta[93], P. Giusti[20a], B.K. Gjelsten[117], L.K. Gladilin[97], C. Glasman[80],
J. Glatzer[48], A. Glazov[42], K.W. Glitza[175], G.L. Glonti[64], J.R. Goddard[75], J. Godfrey[142], J. Godlewski[30], M. Goebel[42],
T. Göpfert[44], C. Goeringer[81], C. Gössling[43], S. Goldfarb[87], T. Golling[176], A. Gomes[124a,b], L.S. Gomez Fajardo[42],
R. Gonçalo[76], J. Goncalves Pinto Firmino Da Costa[42], L. Gonella[21], S. Gonzalez[173], S. González de la Hoz[167],
G. Gonzalez Parra[12], M.L. Gonzalez Silva[27], S. Gonzalez-Sevilla[49], J.J. Goodson[148], L. Goossens[30], P.A. Gorbounov[95],
H.A. Gordon[25], I. Gorelov[103], G. Gorfine[175], B. Gorini[30], E. Gorini[72a,72b], A. Gorišek[74], E. Gornicki[39], B. Gosdzik[42],
A.T. Goshaw[6], M. Gosselink[105], M.I. Gostkin[64], I. Gough Eschrich[163], M. Gouighri[135a], D. Goujdami[135c], M.P. Goulette[49],
A.G. Goussiou[138], C. Goy[5], S. Gozpinar[23], I. Grabowska-Bold[38], P. Grafström[20a,20b], K-J. Grahn[42], F. Grancagnolo[72a],
S. Grancagnolo[16], V. Grassi[148], V. Gratchev[121], N. Grau[35], H.M. Gray[30], J.A. Gray[148], E. Graziani[134a], O.G. Grebenyuk[121],
T. Greenshaw[73], Z.D. Greenwood[25,m], K. Gregersen[36], I.M. Gregor[42], P. Grenier[143], J. Griffiths[8], N. Grigalashvili[64],
A.A. Grillo[137], S. Grinstein[12], Ph. Gris[34], Y.V. Grishkevich[97], J.-F. Grivaz[115], E. Gross[172], J. Grosse-Knetter[54],
J. Groth-Jensen[172], K. Grybel[141], D. Guest[176], C. Guicheney[34], S. Guindon[54], U. Gul[53], H. Guler[85,p], J. Gunther[125],
B. Guo[158], J. Guo[35], P. Gutierrez[111], N. Guttman[153], O. Gutzwiller[173], C. Guyot[136], C. Gwenlan[118], C.B. Gwilliam[73],
A. Haas[143], S. Haas[30], C. Haber[15], H.K. Hadavand[40], D.R. Hadley[18], P. Haefner[21], F. Hahn[30], S. Haider[30], Z. Hajduk[39],
H. Hakobyan[177], D. Hall[118], J. Haller[54], K. Hamacher[175], P. Hamal[113], K. Hamano[86], M. Hamer[54], A. Hamilton[145b,q],
S. Hamilton[161], L. Han[33b], K. Hanagaki[116], K. Hanawa[160], M. Hance[15], C. Handel[81], P. Hanke[58a], J.R. Hansen[36],
J.B. Hansen[36], J.D. Hansen[36], P.H. Hansen[36], P. Hansson[143], K. Hara[160], G.A. Hare[137], T. Harenberg[175], S. Harkusha[90],
D. Harper[87], R.D. Harrington[46], O.M. Harris[138], J. Hartert[48], F. Hartjes[105], T. Haruyama[65], A. Harvey[56], S. Hasegawa[101],
Y. Hasegawa[140], S. Hassani[136], S. Haug[17], M. Hauschild[30], R. Hauser[88], M. Havranek[21], C.M. Hawkes[18], R.J. Hawkings[30],
A.D. Hawkins[79], D. Hawkins[163], T. Hayakawa[66], T. Hayashi[160], D. Hayden[76], C.P. Hays[118], H.S. Hayward[73],
S.J. Haywood[129], M. He[33d], S.J. Head[18], V. Hedberg[79], L. Heelan[8], S. Heim[88], B. Heinemann[15], S. Heisterkamp[36],
L. Helary[22], C. Heller[98], M. Heller[30], S. Hellman[146a,146b], D. Hellmich[21], C. Helsens[12], R.C.W. Henderson[71], M. Henke[58a],
A. Henrichs[54], A.M. Henriques Correia[30], S. Henrot-Versille[115], C. Hensel[54], T. Henß[175], C.M. Hernandez[8],
Y. Hernández Jiménez[167], R. Herrberg[16], G. Herten[48], R. Hertenberger[98], L. Hervas[30], G.G. Hesketh[77], N.P. Hessey[105],
E. Higón-Rodriguez[167], J.C. Hill[28], K.H. Hiller[42], S. Hillert[21], S.J. Hillier[18], I. Hinchliffe[15], E. Hines[120], M. Hirose[116],
F. Hirsch[43], D. Hirschbuehl[175], J. Hobbs[148], N. Hod[153], M.C. Hodgkinson[139], P. Hodgson[139], A. Hoecker[30],
M.R. Hoeferkamp[103], J. Hoffman[40], D. Hoffmann[83], M. Hohlfeld[81], M. Holder[141], S.O. Holmgren[146a], T. Holy[127],
J.L. Holzbauer[88], T.M. Hong[120], L. Hooft van Huysduynen[108], S. Horner[48], J-Y. Hostachy[55], S. Hou[151], A. Hoummada[135a],
J. Howard[118], J. Howarth[82], I. Hristova[16], J. Hrivnac[115], T. Hryn'ova[5], P.J. Hsu[81], S.-C. Hsu[15], D. Hu[35], Z. Hubacek[127],
F. Hubaut[83], F. Huegging[21], A. Huettmann[42], T.B. Huffman[118], E.W. Hughes[35], G. Hughes[71], M. Huhtinen[30],
M. Hurwitz[15], U. Husemann[42], N. Huseynov[64,r], J. Huston[88], J. Huth[57], G. Iacobucci[49], G. Iakovidis[10], M. Ibbotson[82],
I. Ibragimov[141], L. Iconomidou-Fayard[115], J. Idarraga[115], P. Iengo[102a], O. Igonkina[105], Y. Ikegami[65], M. Ikeno[65],

D. Iliadis[154], N. Ilic[158], T. Ince[21], J. Inigo-Golfin[30], P. Ioannou[9], M. Iodice[134a], K. Iordanidou[9], V. Ippolito[132a,132b],
A. Irles Quiles[167], C. Isaksson[166], M. Ishino[67], M. Ishitsuka[157], R. Ishmukhametov[40], C. Issever[118], S. Istin[19a],
A.V. Ivashin[128], W. Iwanski[39], H. Iwasaki[65], J.M. Izen[41], V. Izzo[102a], B. Jackson[120], J.N. Jackson[73], P. Jackson[1],
M.R. Jaekel[30], V. Jain[60], K. Jakobs[48], S. Jakobsen[36], T. Jakoubek[125], J. Jakubek[127], D.K. Jana[111], E. Jansen[77], H. Jansen[30],
A. Jantsch[99], M. Janus[48], G. Jarlskog[79], L. Jeanty[57], I. Jen-La Plante[31], D. Jennens[86], P. Jenni[30], A.E. Loevschall-Jensen[36],
P. Jež[36], S. Jézéquel[5], M.K. Jha[20a], H. Ji[173], W. Ji[81], J. Jia[148], Y. Jiang[33b], M. Jimenez Belenguer[42], S. Jin[33a],
O. Jinnouchi[157], M.D. Joergensen[36], D. Joffe[40], D. Johansen[146a,146b], K.E. Johansson[146a], P. Johansson[139], S. Johnert[42],
K.A. Johns[7], K. Jon-And[146a,146b], G. Jones[170], R.W.L. Jones[71], T.J. Jones[73], C. Joram[30], P.M. Jorge[124a], K.D. Joshi[82],
J. Jovicevic[147], T. Jovin[13b], X. Ju[173], C.A. Jung[43], R.M. Jungst[30], V. Juranek[125], P. Jussel[61], A. Juste Rozas[12], S. Kabana[17],
M. Kaci[167], A. Kaczmarska[39], P. Kadlecik[36], M. Kado[115], H. Kagan[109], M. Kagan[57], E. Kajomovitz[152], S. Kalinin[175],
L.V. Kalinovskaya[64], S. Kama[40], N. Kanaya[155], M. Kaneda[30], S. Kaneti[28], T. Kanno[157], V.A. Kantserov[96], J. Kanzaki[65],
B. Kaplan[108], A. Kapliy[31], J. Kaplon[30], D. Kar[53], M. Karagounis[21], K. Karakostas[10], M. Karnevskiy[42], V. Kartvelishvili[71],
A.N. Karyukhin[128], L. Kashif[173], G. Kasieczka[58b], R.D. Kass[109], A. Kastanas[14], M. Kataoka[5], Y. Kataoka[155],
E. Katsoufis[10], J. Katzy[42], V. Kaushik[7], K. Kawagoe[69], T. Kawamoto[155], G. Kawamura[81], M.S. Kayl[105], S. Kazama[155],
V.A. Kazanin[107], M.Y. Kazarinov[64], R. Keeler[169], P.T. Keener[120], R. Kehoe[40], M. Keil[54], G.D. Kekelidze[64], J.S. Keller[138],
M. Kenyon[53], O. Kepka[125], N. Kerschen[30], B.P. Kerševan[74], S. Kersten[175], K. Kessoku[155], J. Keung[158], F. Khalil-zada[11],
H. Khandanyan[146a,146b], A. Khanov[112], D. Kharchenko[64], A. Khodinov[96], A. Khomich[58a], T.J. Khoo[28], G. Khoriauli[21],
A. Khoroshilov[175], V. Khovanskiy[95], E. Khramov[64], J. Khubua[51b], H. Kim[146a,146b], S.H. Kim[160], N. Kimura[171], O. Kind[16],
B.T. King[73], M. King[66], R.S.B. King[118], J. Kirk[129], A.E. Kiryunin[99], T. Kishimoto[66], D. Kisielewska[38], T. Kitamura[66],
T. Kittelmann[123], K. Kiuchi[160], E. Kladiva[144b], M. Klein[73], U. Klein[73], K. Kleinknecht[81], M. Klemetti[85], A. Klier[172],
P. Klimek[146a,146b], A. Klimentov[25], R. Klingenberg[43], J.A. Klinger[82], E.B. Klinkby[36], T. Klioutchnikova[30], P.F. Klok[104],
S. Klous[105], E.-E. Kluge[58a], T. Kluge[73], P. Kluit[105], S. Kluth[99], N.S. Knecht[158], E. Kneringer[61], E.B.F.G. Knoops[83],
A. Knue[54], B.R. Ko[45], T. Kobayashi[155], M. Kobel[44], M. Kocian[143], P. Kodys[126], K. Köneke[30], A.C. König[104], S. Koenig[81],
L. Köpke[81], F. Koetsveld[104], P. Koevesarki[21], T. Koffas[29], E. Koffeman[105], L.A. Kogan[118], S. Kohlmann[175], F. Kohn[54],
Z. Kohout[127], T. Kohriki[65], T. Koi[143], G.M. Kolachev[107,*], H. Kolanoski[16], V. Kolesnikov[64], I. Koletsou[89a], J. Koll[88],
M. Kollefrath[48], A.A. Komar[94], Y. Komori[155], T. Kondo[65], T. Kono[42,s], A.I. Kononov[48], R. Konoplich[108,t],
N. Konstantinidis[77], S. Koperny[38], K. Korcyl[39], K. Kordas[154], A. Korn[118], A. Korol[107], I. Korolkov[12], E.V. Korolkova[139],
V.A. Korotkov[128], O. Kortner[99], S. Kortner[99], V.V. Kostyukhin[21], S. Kotov[99], V.M. Kotov[64], A. Kotwal[45],
C. Kourkoumelis[9], V. Kouskoura[154], A. Koutsman[159a], R. Kowalewski[169], T.Z. Kowalski[38], W. Kozanecki[136],
A.S. Kozhin[128], V. Kral[127], V.A. Kramarenko[97], G. Kramberger[74], M.W. Krasny[78], A. Krasznahorkay[108], J.K. Kraus[21],
S. Kreiss[108], F. Krejci[127], J. Kretzschmar[73], N. Krieger[54], P. Krieger[158], K. Kroeninger[54], H. Kroha[99], J. Kroll[120],
J. Kroseberg[21], J. Krstic[13a], U. Kruchonak[64], H. Krüger[21], T. Kruker[17], N. Krumnack[63], Z.V. Krumshteyn[64], T. Kubota[86],
S. Kuday[4a], S. Kuehn[48], A. Kugel[58c], T. Kuhl[42], D. Kuhn[61], V. Kukhtin[64], Y. Kulchitsky[90], S. Kuleshov[32b], C. Kummer[98],
M. Kuna[78], J. Kunkle[120], A. Kupco[125], H. Kurashige[66], M. Kurata[160], Y.A. Kurochkin[90], V. Kus[125], E.S. Kuwertz[147],
M. Kuze[157], J. Kvita[142], R. Kwee[16], A. La Rosa[49], L. La Rotonda[37a,37b], L. Labarga[80], J. Labbe[5], S. Lablak[135a],
C. Lacasta[167], F. Lacava[132a,132b], H. Lacker[16], D. Lacour[78], V.R. Lacuesta[167], E. Ladygin[64], R. Lafaye[5], B. Laforge[78],
T. Lagouri[80], S. Lai[48], E. Laisne[55], M. Lamanna[30], L. Lambourne[77], C.L. Lampen[7], W. Lampl[7], E. Lancon[136],
U. Landgraf[48], M.P.J. Landon[75], J.L. Lane[82], V.S. Lang[58a], C. Lange[42], A.J. Lankford[163], F. Lanni[25], K. Lantzsch[175],
S. Laplace[78], C. Lapoire[21], J.F. Laporte[136], T. Lari[89a], A. Larner[118], M. Lassnig[30], P. Laurelli[47], V. Lavorini[37a,37b],
W. Lavrijsen[15], P. Laycock[73], O. Le Dortz[78], E. Le Guirriec[83], C. Le Maner[158], E. Le Menedeu[12], T. LeCompte[6],
F. Ledroit-Guillon[55], H. Lee[105], J.S.H. Lee[116], S.C. Lee[151], L. Lee[176], M. Lefebvre[169], M. Legendre[136], F. Legger[98],
C. Leggett[15], M. Lehmacher[21], G. Lehmann Miotto[30], M.A.L. Leite[24d], R. Leitner[126], D. Lellouch[172], B. Lemmer[54],
V. Lendermann[58a], K.J.C. Leney[145b], T. Lenz[105], G. Lenzen[175], B. Lenzi[30], K. Leonhardt[44], S. Leontsinis[10], F. Lepold[58a],
C. Leroy[93], J-R. Lessard[169], C.G. Lester[28], C.M. Lester[120], J. Levêque[5], D. Levin[87], L.J. Levinson[172], A. Lewis[118],
G.H. Lewis[108], A.M. Leyko[21], M. Leyton[16], B. Li[83], H. Li[173,u], S. Li[33b,v], X. Li[87], Z. Liang[118,w], H. Liao[34], B. Liberti[133a],
P. Lichard[30], M. Lichtnecker[98], K. Lie[165], W. Liebig[14], C. Limbach[21], A. Limosani[86], M. Limper[62], S.C. Lin[151,x],
F. Linde[105], J.T. Linnemann[88], E. Lipeles[120], A. Lipniacka[14], T.M. Liss[165], D. Lissauer[25], A. Lister[49], A.M. Litke[137],
C. Liu[29], D. Liu[151], H. Liu[87], J.B. Liu[87], L. Liu[87], M. Liu[33b], Y. Liu[33b], M. Livan[119a,119b], S.S.A. Livermore[118], A. Lleres[55],
J. Llorente Merino[80], S.L. Lloyd[75], E. Lobodzinska[42], P. Loch[7], W.S. Lockman[137], T. Loddenkoetter[21], F.K. Loebinger[82],
A. Loginov[176], C.W. Loh[168], T. Lohse[16], K. Lohwasser[48], M. Lokajicek[125], V.P. Lombardo[5], R.E. Long[71], L. Lopes[124a],
D. Lopez Mateos[57], J. Lorenz[98], N. Lorenzo Martinez[115], M. Losada[162], P. Loscutoff[15], F. Lo Sterzo[132a,132b],
M.J. Losty[159a,*], X. Lou[41], A. Lounis[115], K.F. Loureiro[162], J. Love[6], P.A. Love[71], A.J. Lowe[143,e], F. Lu[33a], H.J. Lubatti[138],
C. Luci[132a,132b], A. Lucotte[55], A. Ludwig[44], D. Ludwig[42], I. Ludwig[48], J. Ludwig[48], F. Luehring[60], G. Luijckx[105],

W. Lukas[61], D. Lumb[48], L. Luminari[132a], E. Lund[117], B. Lund-Jensen[147], B. Lundberg[79], J. Lundberg[146a,146b],
O. Lundberg[146a,146b], J. Lundquist[36], M. Lungwitz[81], D. Lynn[25], E. Lytken[79], H. Ma[25], L.L. Ma[173], G. Maccarrone[47],
A. Macchiolo[99], B. Maček[74], J. Machado Miguens[124a], R. Mackeprang[36], R.J. Madaras[15], H.J. Maddocks[71], W.F. Mader[44],
R. Maenner[58c], T. Maeno[25], P. Mättig[175], S. Mättig[81], L. Magnoni[163], E. Magradze[54], K. Mahboubi[48], S. Mahmoud[73],
G. Mahout[18], C. Maiani[136], C. Maidantchik[24a], A. Maio[124a,b], S. Majewski[25], Y. Makida[65], N. Makovec[115], P. Mal[136],
B. Malaescu[30], Pa. Malecki[39], P. Malecki[39], V.P. Maleev[121], F. Malek[55], U. Mallik[62], D. Malon[6], C. Malone[143],
S. Maltezos[10], V. Malyshev[107], S. Malyukov[30], R. Mameghani[98], J. Mamuzic[13b], A. Manabe[65], L. Mandelli[89a],
I. Mandić[74], R. Mandrysch[16], J. Maneira[124a], A. Manfredini[99], P.S. Mangeard[88], L. Manhaes de Andrade Filho[24b],
J.A. Manjarres Ramos[136], A. Mann[54], P.M. Manning[137], A. Manousakis-Katsikakis[9], B. Mansoulie[136], A. Mapelli[30],
L. Mapelli[30], L. March[80], J.F. Marchand[29], F. Marchese[133a,133b], G. Marchiori[78], M. Marcisovsky[125], C.P. Marino[169],
F. Marroquim[24a], Z. Marshall[30], F.K. Martens[158], L.F. Marti[17], S. Marti-Garcia[167], B. Martin[30], B. Martin[88], J.P. Martin[93],
T.A. Martin[18], V.J. Martin[46], B. Martin dit Latour[49], S. Martin-Haugh[149], M. Martinez[12], V. Martinez Outschoorn[57],
A.C. Martyniuk[169], M. Marx[82], F. Marzano[132a], A. Marzin[111], L. Masetti[81], T. Mashimo[155], R. Mashinistov[94], J. Masik[82],
A.L. Maslennikov[107], I. Massa[20a,20b], G. Massaro[105], N. Massol[5], P. Mastrandrea[148], A. Mastroberardino[37a,37b],
T. Masubuchi[155], P. Matricon[115], H. Matsunaga[155], T. Matsushita[66], C. Mattravers[118,c], J. Maurer[83], S.J. Maxfield[73],
A. Mayne[139], R. Mazini[151], M. Mazur[21], L. Mazzaferro[133a,133b], M. Mazzanti[89a], J. Mc Donald[85], S.P. Mc Kee[87],
A. McCarn[165], R.L. McCarthy[148], T.G. McCarthy[29], N.A. McCubbin[129], K.W. McFarlane[56,*], J.A. Mcfayden[139],
G. Mchedlidze[51b], T. Mclaughlan[18], S.J. McMahon[129], R.A. McPherson[169,k], A. Meade[84], J. Mechnich[105], M. Mechtel[175],
M. Medinnis[42], R. Meera-Lebbai[111], T. Meguro[116], R. Mehdiyev[93], S. Mehlhase[36], A. Mehta[73], K. Meier[58a], B. Meirose[79],
C. Melachrinos[31], B.R. Mellado Garcia[173], F. Meloni[89a,89b], L. Mendoza Navas[162], Z. Meng[151,u], A. Mengarelli[20a,20b],
S. Menke[99], E. Meoni[161], K.M. Mercurio[57], P. Mermod[49], L. Merola[102a,102b], C. Meroni[89a], F.S. Merritt[31], H. Merritt[109],
A. Messina[30,y], J. Metcalfe[25], A.S. Mete[163], C. Meyer[81], C. Meyer[31], J-P. Meyer[136], J. Meyer[174], J. Meyer[54], T.C. Meyer[30],
J. Miao[33d], S. Michal[30], L. Micu[26a], R.P. Middleton[129], S. Migas[73], L. Mijović[136], G. Mikenberg[172], M. Mikestikova[125],
M. Mikuž[74], D.W. Miller[31], R.J. Miller[88], W.J. Mills[168], C. Mills[57], A. Milov[172], D.A. Milstead[146a,146b], D. Milstein[172],
A.A. Minaenko[128], M. Miñano Moya[167], I.A. Minashvili[64], A.I. Mincer[108], B. Mindur[38], M. Mineev[64], Y. Ming[173],
L.M. Mir[12], G. Mirabelli[132a], J. Mitrevski[137], V.A. Mitsou[167], S. Mitsui[65], P.S. Miyagawa[139], J.U. Mjörnmark[79],
T. Moa[146a,146b], V. Moeller[28], K. Mönig[42], N. Möser[21], S. Mohapatra[148], W. Mohr[48], R. Moles-Valls[167], A. Molfetas[30],
J. Monk[77], E. Monnier[83], J. Montejo Berlingen[12], F. Monticelli[70], S. Monzani[20a,20b], R.W. Moore[3], G.F. Moorhead[86],
C. Mora Herrera[49], A. Moraes[53], N. Morange[136], J. Morel[54], G. Morello[37a,37b], D. Moreno[81], M. Moreno Llácer[167],
P. Morettini[50a], M. Morgenstern[44], M. Morii[57], A.K. Morley[30], G. Mornacchi[30], J.D. Morris[75], L. Morvaj[101],
H.G. Moser[99], M. Mosidze[51b], J. Moss[109], R. Mount[143], E. Mountricha[10,z], S.V. Mouraviev[94,*], E.J.W. Moyse[84],
F. Mueller[58a], J. Mueller[123], K. Mueller[21], T.A. Müller[98], T. Mueller[81], D. Muenstermann[30], Y. Munwes[153],
W.J. Murray[129], I. Mussche[105], E. Musto[102a,102b], A.G. Myagkov[128], M. Myska[125], J. Nadal[12], K. Nagai[160], R. Nagai[157],
K. Nagano[65], A. Nagarkar[109], Y. Nagasaka[59], M. Nagel[99], A.M. Nairz[30], Y. Nakahama[30], K. Nakamura[155],
T. Nakamura[155], I. Nakano[110], G. Nanava[21], A. Napier[161], R. Narayan[58b], M. Nash[77,c], T. Nattermann[21], T. Naumann[42],
G. Navarro[162], H.A. Neal[87], P.Yu. Nechaeva[94], T.J. Neep[82], A. Negri[119a,119b], G. Negri[30], S. Nektarijevic[49],
A. Nelson[163], T.K. Nelson[143], S. Nemecek[125], P. Nemethy[108], A.A. Nepomuceno[24a], M. Nessi[30,aa], M.S. Neubauer[165],
M. Neumann[175], A. Neusiedl[81], R.M. Neves[108], P. Nevski[25], F.M. Newcomer[120], P.R. Newman[18], V. Nguyen Thi Hong[136],
R.B. Nickerson[118], R. Nicolaidou[136], B. Nicquevert[30], F. Niedercorn[115], J. Nielsen[137], N. Nikiforou[35], A. Nikiforov[16],
V. Nikolaenko[128], I. Nikolic-Audit[78], K. Nikolics[49], K. Nikolopoulos[18], H. Nilsen[48], P. Nilsson[8], Y. Ninomiya[155],
A. Nisati[132a], R. Nisius[99], T. Nobe[157], L. Nodulman[6], M. Nomachi[116], I. Nomidis[154], S. Norberg[111], M. Nordberg[30],
P.R. Norton[129], J. Novakova[126], M. Nozaki[65], L. Nozka[113], I.M. Nugent[159a], A.-E. Nuncio-Quiroz[21],
G. Nunes Hanninger[86], T. Nunnemann[98], E. Nurse[77], B.J. O'Brien[46], S.W. O'Neale[18,*], D.C. O'Neil[142], V. O'Shea[53],
L.B. Oakes[98], F.G. Oakham[29,d], H. Oberlack[99], J. Ocariz[78], A. Ochi[66], S. Oda[69], S. Odaka[65], J. Odier[83], H. Ogren[60],
A. Oh[82], S.H. Oh[45], C.C. Ohm[30], T. Ohshima[101], H. Okawa[25], Y. Okumura[31], T. Okuyama[155], A. Olariu[26a],
A.G. Olchevski[64], S.A. Olivares Pino[32a], M. Oliveira[124a,h], D. Oliveira Damazio[25], E. Oliver Garcia[167], D. Olivito[120],
A. Olszewski[39], J. Olszowska[39], A. Onofre[124a,ab], P.U.E. Onyisi[31], C.J. Oram[159a], M.J. Oreglia[31], Y. Oren[153],
D. Orestano[134a,134b], N. Orlando[72a,72b], I. Orlov[107], C. Oropeza Barrera[53], R.S. Orr[158], B. Osculati[50a,50b], R. Ospanov[120],
C. Osuna[12], G. Otero y Garzon[27], J.P. Ottersbach[105], M. Ouchrif[135d], E.A. Ouellette[169], F. Ould-Saada[117], A. Ouraou[136],
Q. Ouyang[33a], A. Ovcharova[15], M. Owen[82], S. Owen[139], V.E. Ozcan[19a], N. Ozturk[8], A. Pacheco Pages[12],
C. Padilla Aranda[12], S. Pagan Griso[15], E. Paganis[139], C. Pahl[99], F. Paige[25], P. Pais[84], K. Pajchel[117], G. Palacino[159b],
C.P. Paleari[7], S. Palestini[30], D. Pallin[34], A. Palma[124a], J.D. Palmer[18], Y.B. Pan[173], E. Panagiotopoulou[10], P. Pani[105],
N. Panikashvili[87], S. Panitkin[25], D. Pantea[26a], A. Papadelis[146a], Th.D. Papadopoulou[10], A. Paramonov[6],

D. Paredes Hernandez[34], W. Park[25,ac], M.A. Parker[28], F. Parodi[50a,50b], J.A. Parsons[35], U. Parzefall[48], S. Pashapour[54],
E. Pasqualucci[132a], S. Passaggio[50a], A. Passeri[134a], F. Pastore[134a,134b,∗], Fr. Pastore[76], G. Pásztor[49,ad], S. Pataraia[175],
N. Patel[150], J.R. Pater[82], S. Patricelli[102a,102b], T. Pauly[30], M. Pecsy[144a], S. Pedraza Lopez[167], M.I. Pedraza Morales[173],
S.V. Peleganchuk[107], D. Pelikan[166], H. Peng[33b], B. Penning[31], A. Penson[35], J. Penwell[60], M. Perantoni[24a], K. Perez[35,ae],
T. Perez Cavalcanti[42], E. Perez Codina[159a], M.T. Pérez García-Estañ[167], V. Perez Reale[35], L. Perini[89a,89b], H. Pernegger[30],
R. Perrino[72a], P. Perrodo[5], V.D. Peshekhonov[64], K. Peters[30], B.A. Petersen[30], J. Petersen[30], T.C. Petersen[36], E. Petit[5],
A. Petridis[154], C. Petridou[154], E. Petrolo[132a], F. Petrucci[134a,134b], D. Petschull[42], M. Petteni[142], R. Pezoa[32b], A. Phan[86],
P.W. Phillips[129], G. Piacquadio[30], A. Picazio[49], E. Piccaro[75], M. Piccinini[20a,20b], S.M. Piec[42], R. Piegaia[27], D.T. Pignotti[109],
J.E. Pilcher[31], A.D. Pilkington[82], J. Pina[124a,b], M. Pinamonti[164a,164c], A. Pinder[118], J.L. Pinfold[3], B. Pinto[124a],
C. Pizio[89a,89b], M. Plamondon[169], M.-A. Pleier[25], E. Plotnikova[64], A. Poblaguev[25], S. Poddar[58a], F. Podlyski[34],
L. Poggioli[115], D. Pohl[21], M. Pohl[49], G. Polesello[119a], A. Policicchio[37a,37b], A. Polini[20a], J. Poll[75], V. Polychronakos[25],
D. Pomeroy[23], K. Pommès[30], L. Pontecorvo[132a], B.G. Pope[88], G.A. Popeneciu[26a], D.S. Popovic[13a], A. Poppleton[30],
X. Portell Bueso[30], G.E. Pospelov[99], S. Pospisil[127], I.N. Potrap[99], C.J. Potter[149], C.T. Potter[114], G. Poulard[30], J. Poveda[60],
V. Pozdnyakov[64], R. Prabhu[77], P. Pralavorio[83], A. Pranko[15], S. Prasad[30], R. Pravahan[25], S. Prell[63], K. Pretzl[17], D. Price[60],
J. Price[73], L.E. Price[6], D. Prieur[123], M. Primavera[72a], K. Prokofiev[108], F. Prokoshin[32b], S. Protopopescu[25], J. Proudfoot[6],
X. Prudent[44], M. Przybycien[38], H. Przysiezniak[5], S. Psoroulas[21], E. Ptacek[114], E. Pueschel[84], J. Purdham[87],
M. Purohit[25,ac], P. Puzo[115], Y. Pylypchenko[62], J. Qian[87], A. Quadt[54], D.R. Quarrie[15], W.B. Quayle[173], F. Quinonez[32a],
M. Raas[104], V. Radeka[25], V. Radescu[42], P. Radloff[114], T. Rador[19a], F. Ragusa[89a,89b], G. Rahal[178], A.M. Rahimi[109],
D. Rahm[25], S. Rajagopalan[25], M. Rammensee[48], M. Rammes[141], A.S. Randle-Conde[40], K. Randrianarivony[29],
F. Rauscher[98], T.C. Rave[48], M. Raymond[30], A.L. Read[117], D.M. Rebuzzi[119a,119b], A. Redelbach[174], G. Redlinger[25],
R. Reece[120], K. Reeves[41], E. Reinherz-Aronis[153], A. Reinsch[114], I. Reisinger[43], C. Rembser[30], Z.L. Ren[151], A. Renaud[115],
M. Rescigno[132a], S. Resconi[89a], B. Resende[136], P. Reznicek[98], R. Rezvani[158], R. Richter[99], E. Richter-Was[5,af], M. Ridel[78],
M. Rijpstra[105], M. Rijssenbeek[148], A. Rimoldi[119a,119b], L. Rinaldi[20a], R.R. Rios[40], I. Riu[12], G. Rivoltella[89a,89b],
F. Rizatdinova[112], E. Rizvi[75], S.H. Robertson[85,k], A. Robichaud-Veronneau[118], D. Robinson[28], J.E.M. Robinson[82],
A. Robson[53], J.G. Rocha de Lima[106], C. Roda[122a,122b], D. Roda Dos Santos[30], A. Roe[54], S. Roe[30], O. Røhne[117], S. Rolli[161],
A. Romaniouk[96], M. Romano[20a,20b], G. Romeo[27], E. Romero Adam[167], N. Rompotis[138], L. Roos[78], E. Ros[167],
S. Rosati[132a], K. Rosbach[49], A. Rose[149], M. Rose[76], G.A. Rosenbaum[158], E.I. Rosenberg[63], P.L. Rosendahl[14],
O. Rosenthal[141], L. Rosselet[49], V. Rossetti[12], E. Rossi[132a,132b], L.P. Rossi[50a], M. Rotaru[26a], I. Roth[172], J. Rothberg[138],
D. Rousseau[115], C.R. Royon[136], A. Rozanov[83], Y. Rozen[152], X. Ruan[33a,ag], F. Rubbo[12], I. Rubinskiy[42], N. Ruckstuhl[105],
V.I. Rud[97], C. Rudolph[44], G. Rudolph[61], F. Rühr[7], A. Ruiz-Martinez[63], L. Rumyantsev[64], Z. Rurikova[48],
N.A. Rusakovich[64], J.P. Rutherfoord[7], C. Ruwiedel[15,∗], P. Ruzicka[125], Y.F. Ryabov[121], M. Rybar[126], G. Rybkin[115],
N.C. Ryder[118], A.F. Saavedra[150], I. Sadeh[153], H.F-W. Sadrozinski[137], R. Sadykov[64], F. Safai Tehrani[132a], H. Sakamoto[155],
G. Salamanna[75], A. Salamon[133a], M. Saleem[111], D. Salek[30], D. Salihagic[99], A. Salnikov[143], J. Salt[167],
B.M. Salvachua Ferrando[6], D. Salvatore[37a,37b], F. Salvatore[149], A. Salvucci[104], A. Salzburger[30], D. Sampsonidis[154],
B.H. Samset[117], A. Sanchez[102a,102b], V. Sanchez Martinez[167], H. Sandaker[14], H.G. Sander[81], M.P. Sanders[98],
M. Sandhoff[175], T. Sandoval[28], C. Sandoval[162], R. Sandstroem[99], D.P.C. Sankey[129], A. Sansoni[47], C. Santamarina Rios[85],
C. Santoni[34], R. Santonico[133a,133b], H. Santos[124a], J.G. Saraiva[124a], T. Sarangi[173], E. Sarkisyan-Grinbaum[8], F. Sarri[122a,122b],
G. Sartisohn[175], O. Sasaki[65], Y. Sasaki[155], N. Sasao[67], I. Satsounkevitch[90], G. Sauvage[5,∗], E. Sauvan[5], J.B. Sauvan[115],
P. Savard[158,d], V. Savinov[123], D.O. Savu[30], L. Sawyer[25,m], D.H. Saxon[53], J. Saxon[120], C. Sbarra[20a], A. Sbrizzi[20a,20b],
D.A. Scannicchio[163], M. Scarcella[150], J. Schaarschmidt[115], P. Schacht[99], D. Schaefer[120], U. Schäfer[81], S. Schaepe[21],
S. Schaetzel[58b], A.C. Schaffer[115], D. Schaile[98], R.D. Schamberger[148], A.G. Schamov[107], V. Scharf[58a], V.A. Schegelsky[121],
D. Scheirich[87], M. Schernau[163], M.I. Scherzer[35], C. Schiavi[50a,50b], J. Schieck[98], M. Schioppa[37a,37b], S. Schlenker[30],
E. Schmidt[48], K. Schmieden[21], C. Schmitt[81], S. Schmitt[58b], M. Schmitz[21], B. Schneider[17], U. Schnoor[44], A. Schoening[58b],
A.L.S. Schorlemmer[54], M. Schott[30], D. Schouten[159a], J. Schovancova[125], M. Schram[85], C. Schroeder[81], N. Schroer[58c],
M.J. Schultens[21], J. Schultes[175], H.-C. Schultz-Coulon[58a], H. Schulz[16], M. Schumacher[48], B.A. Schumm[137],
Ph. Schune[136], C. Schwanenberger[82], A. Schwartzman[143], Ph. Schwegler[99], Ph. Schwemling[78], R. Schwienhorst[88],
R. Schwierz[44], J. Schwindling[136], T. Schwindt[21], M. Schwoerer[5], G. Sciolla[23], W.G. Scott[129], J. Searcy[114], G. Sedov[42],
E. Sedykh[121], S.C. Seidel[103], A. Seiden[137], F. Seifert[44], J.M. Seixas[24a], G. Sekhniaidze[102a], S.J. Sekula[40], K.E. Selbach[46],
D.M. Seliverstov[121], B. Sellden[146a], G. Sellers[73], M. Seman[144b], N. Semprini-Cesari[20a,20b], C. Serfon[98], L. Serin[115],
L. Serkin[54], R. Seuster[99], H. Severini[111], A. Sfyrla[30], E. Shabalina[54], M. Shamim[114], L.Y. Shan[33a], J.T. Shank[22],
Q.T. Shao[86], M. Shapiro[15], P.B. Shatalov[95], K. Shaw[164a,164c], D. Sherman[176], P. Sherwood[77], A. Shibata[108], S. Shimizu[101],
M. Shimojima[100], T. Shin[56], M. Shiyakova[64], A. Shmeleva[94], M.J. Shochet[31], D. Short[118], S. Shrestha[63], E. Shulga[96],
M.A. Shupe[7], P. Sicho[125], A. Sidoti[132a], F. Siegert[48], Dj. Sijacki[13a], O. Silbert[172], J. Silva[124a], Y. Silver[153],

D. Silverstein[143], S.B. Silverstein[146a], V. Simak[127], O. Simard[136], Lj. Simic[13a], S. Simion[115], E. Simioni[81], B. Simmons[77],
R. Simoniello[89a,89b], M. Simonyan[36], P. Sinervo[158], N.B. Sinev[114], V. Sipica[141], G. Siragusa[174], A. Sircar[25],
A.N. Sisakyan[64,*], S.Yu. Sivoklokov[97], J. Sjölin[146a,146b], T.B. Sjursen[14], L.A. Skinnari[15], H.P. Skottowe[57], K. Skovpen[107],
P. Skubic[111], M. Slater[18], T. Slavicek[127], K. Sliwa[161], V. Smakhtin[172], B.H. Smart[46], L. Smestad[117], S.Yu. Smirnov[96],
Y. Smirnov[96], L.N. Smirnova[97], O. Smirnova[79], B.C. Smith[57], D. Smith[143], K.M. Smith[53], M. Smizanska[71], K. Smolek[127],
A.A. Snesarev[94], S.W. Snow[82], J. Snow[111], S. Snyder[25], R. Sobie[169,k], J. Sodomka[127], A. Soffer[153], C.A. Solans[167],
M. Solar[127], J. Solc[127], E.Yu. Soldatov[96], U. Soldevila[167], E. Solfaroli Camillocci[132a,132b], A.A. Solodkov[128],
O.V. Solovyanov[128], V. Solovyev[121], N. Soni[1], V. Sopko[127], B. Sopko[127], M. Sosebee[8], R. Soualah[164a,164c],
A. Soukharev[107], S. Spagnolo[72a,72b], F. Spanò[76], R. Spighi[20a], G. Spigo[30], R. Spiwoks[30], M. Spousta[126,ah], T. Spreitzer[158],
B. Spurlock[8], R.D. St. Denis[53], J. Stahlman[120], R. Stamen[58a], E. Stanecka[39], R.W. Stanek[6], C. Stanescu[134a],
M. Stanescu-Bellu[42], M.M. Stanitzki[42], S. Stapnes[117], E.A. Starchenko[128], J. Stark[55], P. Staroba[125], P. Starovoitov[42],
R. Staszewski[39], A. Staude[98], P. Stavina[144a,*], G. Steele[53], P. Steinbach[44], P. Steinberg[25], I. Stekl[127], B. Stelzer[142],
H.J. Stelzer[88], O. Stelzer-Chilton[159a], H. Stenzel[52], S. Stern[99], G.A. Stewart[30], J.A. Stillings[21], M.C. Stockton[85],
K. Stoerig[48], G. Stoicea[26a], S. Stonjek[99], P. Strachota[126], A.R. Stradling[8], A. Straessner[44], J. Strandberg[147],
S. Strandberg[146a,146b], A. Strandlie[117], M. Strang[109], E. Strauss[143], M. Strauss[111], P. Strizenec[144b], R. Ströhmer[174],
D.M. Strom[114], J.A. Strong[76,*], R. Stroynowski[40], J. Strube[129], B. Stugu[14], I. Stumer[25,*], J. Stupak[148], P. Sturm[175],
N.A. Styles[42], D.A. Soh[151,w], D. Su[143], HS. Subramania[3], A. Succurro[12], Y. Sugaya[116], C. Suhr[106], M. Suk[126],
V.V. Sulin[94], S. Sultansoy[4d], T. Sumida[67], X. Sun[55], J.E. Sundermann[48], K. Suruliz[139], G. Susinno[37a,37b], M.R. Sutton[149],
Y. Suzuki[65], Y. Suzuki[66], M. Svatos[125], S. Swedish[168], I. Sykora[144a], T. Sykora[126], J. Sánchez[167], D. Ta[105], K. Tackmann[42],
A. Taffard[163], R. Tafirout[159a], N. Taiblum[153], Y. Takahashi[101], H. Takai[25], R. Takashima[68], H. Takeda[66], T. Takeshita[140],
Y. Takubo[65], M. Talby[83], A. Talyshev[107,f], M.C. Tamsett[25], K.G. Tan[86], J. Tanaka[155], R. Tanaka[115], S. Tanaka[131],
S. Tanaka[65], A.J. Tanasijczuk[142], K. Tani[66], N. Tannoury[83], S. Tapprogge[81], D. Tardif[158], S. Tarem[152], F. Tarrade[29],
G.F. Tartarelli[89a], P. Tas[126], M. Tasevsky[125], E. Tassi[37a,37b], M. Tatarkhanov[15], Y. Tayalati[135d], C. Taylor[77], F.E. Taylor[92],
G.N. Taylor[86], W. Taylor[159b], M. Teinturier[115], F.A. Teischinger[30], M. Teixeira Dias Castanheira[75], P. Teixeira-Dias[76],
K.K. Temming[48], H. Ten Kate[30], P.K. Teng[151], S. Terada[65], K. Terashi[155], J. Terron[80], M. Testa[47], R.J. Teuscher[158,k],
J. Therhaag[21], T. Theveneaux-Pelzer[78], S. Thoma[48], J.P. Thomas[18], E.N. Thompson[35], P.D. Thompson[18],
P.D. Thompson[158], A.S. Thompson[53], L.A. Thomsen[36], E. Thomson[120], M. Thomson[28], W.M. Thong[86], R.P. Thun[87],
F. Tian[35], M.J. Tibbetts[15], T. Tic[125], V.O. Tikhomirov[94], Y.A. Tikhonov[107,f], S. Timoshenko[96], P. Tipton[176], S. Tisserant[83],
T. Todorov[5], S. Todorova-Nova[161], B. Toggerson[163], J. Tojo[69], S. Tokár[144a], K. Tokushuku[65], K. Tollefson[88],
M. Tomoto[101], L. Tompkins[31], K. Toms[103], A. Tonoyan[14], C. Topfel[17], N.D. Topilin[64], I. Torchiani[30], E. Torrence[114],
H. Torres[78], E. Torró Pastor[167], J. Toth[83,ad], F. Touchard[83], D.R. Tovey[139], T. Trefzger[174], L. Tremblet[30], A. Tricoli[30],
I.M. Trigger[159a], S. Trincaz-Duvoid[78], M.F. Tripiana[70], N. Triplett[25], W. Trischuk[158], B. Trocmé[55], C. Troncon[89a],
M. Trottier-McDonald[142], M. Trzebinski[39], A. Trzupek[39], C. Tsarouchas[30], J.C-L. Tseng[118], M. Tsiakiris[105],
P.V. Tsiareshka[90], D. Tsionou[5,ai], G. Tsipolitis[10], S. Tsiskaridze[12], V. Tsiskaridze[48], E.G. Tskhadadze[51a], I.I. Tsukerman[95],
V. Tsulaia[15], J.-W. Tsung[21], S. Tsuno[65], D. Tsybychev[148], A. Tua[139], A. Tudorache[26a], V. Tudorache[26a], J.M. Tuggle[31],
M. Turala[39], D. Turecek[127], I. Turk Cakir[4e], E. Turlay[105], R. Turra[89a,89b], P.M. Tuts[35], A. Tykhonov[74], M. Tylmad[146a,146b],
M. Tyndel[129], G. Tzanakos[9], K. Uchida[21], I. Ueda[155], R. Ueno[29], M. Ugland[14], M. Uhlenbrock[21], M. Uhrmacher[54],
F. Ukegawa[160], G. Unal[30], A. Undrus[25], G. Unel[163], Y. Unno[65], D. Urbaniec[35], G. Usai[8], M. Uslenghi[119a,119b],
L. Vacavant[83], V. Vacek[127], B. Vachon[85], S. Vahsen[15], J. Valenta[125], S. Valentinetti[20a,20b], A. Valero[167], S. Valkar[126],
E. Valladolid Gallego[167], S. Vallecorsa[152], J.A. Valls Ferrer[167], R. Van Berg[120], P.C. Van Der Deijl[105], R. van der Geer[105],
H. van der Graaf[105], R. Van Der Leeuw[105], E. van der Poel[105], D. van der Ster[30], N. van Eldik[30], P. van Gemmeren[6],
I. van Vulpen[105], M. Vanadia[99], W. Vandelli[30], A. Vaniachine[6], P. Vankov[42], F. Vannucci[78], R. Vari[132a], E.W. Varnes[7],
T. Varol[84], D. Varouchas[15], A. Vartapetian[8], K.E. Varvell[150], V.I. Vassilakopoulos[56], F. Vazeille[34], T. Vazquez Schroeder[54],
G. Vegni[89a,89b], J.J. Veillet[115], F. Veloso[124a], R. Veness[30], S. Veneziano[132a], A. Ventura[72a,72b], D. Ventura[84], M. Venturi[48],
N. Venturi[158], V. Vercesi[119a], M. Verducci[138], W. Verkerke[105], J.C. Vermeulen[105], A. Vest[44], M.C. Vetterli[142,d],
I. Vichou[165], T. Vickey[145b,aj], O.E. Vickey Boeriu[145b], G.H.A. Viehhauser[118], S. Viel[168], M. Villa[20a,20b],
M. Villaplana Perez[167], E. Vilucchi[47], M.G. Vincter[29], E. Vinek[30], V.B. Vinogradov[64], M. Virchaux[136,*], J. Virzi[15],
O. Vitells[172], M. Viti[42], I. Vivarelli[48], F. Vives Vaque[3], S. Vlachos[10], D. Vladoiu[98], M. Vlasak[127], A. Vogel[21], P. Vokac[127],
G. Volpi[47], M. Volpi[86], G. Volpini[89a], H. von der Schmitt[99], H. von Radziewski[48], E. von Toerne[21], V. Vorobel[126],
V. Vorwerk[12], M. Vos[167], R. Voss[30], T.T. Voss[175], J.H. Vossebeld[73], N. Vranjes[136], M. Vranjes Milosavljevic[105], V. Vrba[125],
M. Vreeswijk[105], T. Vu Anh[48], R. Vuillermet[30], I. Vukotic[31], W. Wagner[175], P. Wagner[120], H. Wahlen[175], S. Wahrmund[44],
J. Wakabayashi[101], S. Walch[87], J. Walder[71], R. Walker[98], W. Walkowiak[141], R. Wall[176], P. Waller[73], B. Walsh[176],
C. Wang[45], H. Wang[173], H. Wang[33b,ak], J. Wang[151], J. Wang[55], R. Wang[103], S.M. Wang[151], T. Wang[21], A. Warburton[85],

C.P. Ward[28], M. Warsinsky[48], A. Washbrook[46], C. Wasicki[42], I. Watanabe[66], P.M. Watkins[18], A.T. Watson[18], I.J. Watson[150], M.F. Watson[18], G. Watts[138], S. Watts[82], A.T. Waugh[150], B.M. Waugh[77], M.S. Weber[17], P. Weber[54], A.R. Weidberg[118], P. Weigell[99], J. Weingarten[54], C. Weiser[48], P.S. Wells[30], T. Wenaus[25], D. Wendland[16], Z. Weng[151,w], T. Wengler[30], S. Wenig[30], N. Wermes[21], M. Werner[48], P. Werner[30], M. Werth[163], M. Wessels[58a], J. Wetter[161], C. Weydert[55], K. Whalen[29], S.J. Wheeler-Ellis[163], A. White[8], M.J. White[86], S. White[122a,122b], S.R. Whitehead[118], D. Whiteson[163], D. Whittington[60], F. Wicek[115], D. Wicke[175], F.J. Wickens[129], W. Wiedenmann[173], M. Wielers[129], P. Wienemann[21], C. Wiglesworth[75], L.A.M. Wiik-Fuchs[48], P.A. Wijeratne[77], A. Wildauer[99], M.A. Wildt[42,s], I. Wilhelm[126], H.G. Wilkens[30], J.Z. Will[98], E. Williams[35], H.H. Williams[120], W. Willis[35], S. Willocq[84], J.A. Wilson[18], M.G. Wilson[143], A. Wilson[87], I. Wingerter-Seez[5], S. Winkelmann[48], F. Winklmeier[30], M. Wittgen[143], S.J. Wollstadt[81], M.W. Wolter[39], H. Wolters[124a,h], W.C. Wong[41], G. Wooden[87], B.K. Wosiek[39], J. Wotschack[30], M.J. Woudstra[82], K.W. Wozniak[39], K. Wraight[53], M. Wright[53], B. Wrona[73], S.L. Wu[173], X. Wu[49], Y. Wu[33b,al], E. Wulf[35], B.M. Wynne[46], S. Xella[36], M. Xiao[136], S. Xie[48], C. Xu[33b,z], D. Xu[139], B. Yabsley[150], S. Yacoob[145a,am], M. Yamada[65], H. Yamaguchi[155], A. Yamamoto[65], K. Yamamoto[63], S. Yamamoto[155], T. Yamamura[155], T. Yamanaka[155], J. Yamaoka[45], T. Yamazaki[155], Y. Yamazaki[66], Z. Yan[22], H. Yang[87], U.K. Yang[82], Y. Yang[60], Z. Yang[146a,146b], S. Yanush[91], L. Yao[33a], Y. Yao[15], Y. Yasu[65], G.V. Ybeles Smit[130], J. Ye[40], S. Ye[25], M. Yilmaz[4c], R. Yoosoofmiya[123], K. Yorita[171], R. Yoshida[6], C. Young[143], C.J. Young[118], S. Youssef[22], D. Yu[25], J. Yu[8], J. Yu[112], L. Yuan[66], A. Yurkewicz[106], B. Zabinski[39], R. Zaidan[62], A.M. Zaitsev[128], Z. Zajacova[30], L. Zanello[132a,132b], D. Zanzi[99], A. Zaytsev[25], C. Zeitnitz[175], M. Zeman[125], A. Zemla[39], C. Zendler[21], O. Zenin[128], T. Ženiš[144a], Z. Zinonos[122a,122b], S. Zenz[15], D. Zerwas[115], G. Zevi della Porta[57], Z. Zhan[33d], D. Zhang[33b,ak], H. Zhang[88], J. Zhang[6], X. Zhang[33d], Z. Zhang[115], L. Zhao[108], T. Zhao[138], Z. Zhao[33b], A. Zhemchugov[64], J. Zhong[118], B. Zhou[87], N. Zhou[163], Y. Zhou[151], C.G. Zhu[33d], H. Zhu[42], J. Zhu[87], Y. Zhu[33b], X. Zhuang[98], V. Zhuravlov[99], D. Zieminska[60], N.I. Zimin[64], R. Zimmermann[21], S. Zimmermann[21], S. Zimmermann[48], M. Ziolkowski[141], R. Zitoun[5], L. Živković[35], V.V. Zmouchko[128,*], G. Zobernig[173], A. Zoccoli[20a,20b], M. zur Nedden[16], V. Zutshi[106], L. Zwalinski[30].

[1] School of Chemistry and Physics, University of Adelaide, Adelaide, Australia
[2] Physics Department, SUNY Albany, Albany NY, United States of America
[3] Department of Physics, University of Alberta, Edmonton AB, Canada
[4] (a) Department of Physics, Ankara University, Ankara; (b) Department of Physics, Dumlupinar University, Kutahya; (c) Department of Physics, Gazi University, Ankara; (d) Division of Physics, TOBB University of Economics and Technology, Ankara; (e) Turkish Atomic Energy Authority, Ankara, Turkey
[5] LAPP, CNRS/IN2P3 and Université de Savoie, Annecy-le-Vieux, France
[6] High Energy Physics Division, Argonne National Laboratory, Argonne IL, United States of America
[7] Department of Physics, University of Arizona, Tucson AZ, United States of America
[8] Department of Physics, The University of Texas at Arlington, Arlington TX, United States of America
[9] Physics Department, University of Athens, Athens, Greece
[10] Physics Department, National Technical University of Athens, Zografou, Greece
[11] Institute of Physics, Azerbaijan Academy of Sciences, Baku, Azerbaijan
[12] Institut de Física d'Altes Energies and Departament de Física de la Universitat Autònoma de Barcelona and ICREA, Barcelona, Spain
[13] (a) Institute of Physics, University of Belgrade, Belgrade; (b) Vinca Institute of Nuclear Sciences, University of Belgrade, Belgrade, Serbia
[14] Department for Physics and Technology, University of Bergen, Bergen, Norway
[15] Physics Division, Lawrence Berkeley National Laboratory and University of California, Berkeley CA, United States of America
[16] Department of Physics, Humboldt University, Berlin, Germany
[17] Albert Einstein Center for Fundamental Physics and Laboratory for High Energy Physics, University of Bern, Bern, Switzerland
[18] School of Physics and Astronomy, University of Birmingham, Birmingham, United Kingdom
[19] (a) Department of Physics, Bogazici University, Istanbul; (b) Division of Physics, Dogus University, Istanbul; (c) Department of Physics Engineering, Gaziantep University, Gaziantep; (d) Department of Physics, Istanbul Technical University, Istanbul, Turkey
[20] (a) INFN Sezione di Bologna; (b) Dipartimento di Fisica, Università di Bologna, Bologna, Italy
[21] Physikalisches Institut, University of Bonn, Bonn, Germany
[22] Department of Physics, Boston University, Boston MA, United States of America

[23] Department of Physics, Brandeis University, Waltham MA, United States of America

[24] [a] Universidade Federal do Rio De Janeiro COPPE/EE/IF, Rio de Janeiro; [b] Federal University of Juiz de Fora (UFJF), Juiz de Fora; [c] Federal University of Sao Joao del Rei (UFSJ), Sao Joao del Rei; [d] Instituto de Fisica, Universidade de Sao Paulo, Sao Paulo, Brazil

[25] Physics Department, Brookhaven National Laboratory, Upton NY, United States of America

[26] [a] National Institute of Physics and Nuclear Engineering, Bucharest; [b] University Politehnica Bucharest, Bucharest; [c] West University in Timisoara, Timisoara, Romania

[27] Departamento de Física, Universidad de Buenos Aires, Buenos Aires, Argentina

[28] Cavendish Laboratory, University of Cambridge, Cambridge, United Kingdom

[29] Department of Physics, Carleton University, Ottawa ON, Canada

[30] CERN, Geneva, Switzerland

[31] Enrico Fermi Institute, University of Chicago, Chicago IL, United States of America

[32] [a] Departamento de Física, Pontificia Universidad Católica de Chile, Santiago; [b] Departamento de Física, Universidad Técnica Federico Santa María, Valparaíso, Chile

[33] [a] Institute of High Energy Physics, Chinese Academy of Sciences, Beijing; [b] Department of Modern Physics, University of Science and Technology of China, Anhui; [c] Department of Physics, Nanjing University, Jiangsu; [d] School of Physics, Shandong University, Shandong, China

[34] Laboratoire de Physique Corpusculaire, Clermont Université and Université Blaise Pascal and CNRS/IN2P3, Clermont-Ferrand, France

[35] Nevis Laboratory, Columbia University, Irvington NY, United States of America

[36] Niels Bohr Institute, University of Copenhagen, Kobenhavn, Denmark

[37] [a] INFN Gruppo Collegato di Cosenza; [b] Dipartimento di Fisica, Università della Calabria, Arcavata di Rende, Italy

[38] AGH University of Science and Technology, Faculty of Physics and Applied Computer Science, Krakow, Poland

[39] The Henryk Niewodniczanski Institute of Nuclear Physics, Polish Academy of Sciences, Krakow, Poland

[40] Physics Department, Southern Methodist University, Dallas TX, United States of America

[41] Physics Department, University of Texas at Dallas, Richardson TX, United States of America

[42] DESY, Hamburg and Zeuthen, Germany

[43] Institut für Experimentelle Physik IV, Technische Universität Dortmund, Dortmund, Germany

[44] Institut für Kern- und Teilchenphysik, Technical University Dresden, Dresden, Germany

[45] Department of Physics, Duke University, Durham NC, United States of America

[46] SUPA - School of Physics and Astronomy, University of Edinburgh, Edinburgh, United Kingdom

[47] INFN Laboratori Nazionali di Frascati, Frascati, Italy

[48] Fakultät für Mathematik und Physik, Albert-Ludwigs-Universität, Freiburg, Germany

[49] Section de Physique, Université de Genève, Geneva, Switzerland

[50] [a] INFN Sezione di Genova; [b] Dipartimento di Fisica, Università di Genova, Genova, Italy

[51] [a] E. Andronikashvili Institute of Physics, Iv. Javakhishvili Tbilisi State University, Tbilisi; [b] High Energy Physics Institute, Tbilisi State University, Tbilisi, Georgia

[52] II Physikalisches Institut, Justus-Liebig-Universität Giessen, Giessen, Germany

[53] SUPA - School of Physics and Astronomy, University of Glasgow, Glasgow, United Kingdom

[54] II Physikalisches Institut, Georg-August-Universität, Göttingen, Germany

[55] Laboratoire de Physique Subatomique et de Cosmologie, Université Joseph Fourier and CNRS/IN2P3 and Institut National Polytechnique de Grenoble, Grenoble, France

[56] Department of Physics, Hampton University, Hampton VA, United States of America

[57] Laboratory for Particle Physics and Cosmology, Harvard University, Cambridge MA, United States of America

[58] [a] Kirchhoff-Institut für Physik, Ruprecht-Karls-Universität Heidelberg, Heidelberg; [b] Physikalisches Institut, Ruprecht-Karls-Universität Heidelberg, Heidelberg; [c] ZITI Institut für technische Informatik, Ruprecht-Karls-Universität Heidelberg, Mannheim, Germany

[59] Faculty of Applied Information Science, Hiroshima Institute of Technology, Hiroshima, Japan

[60] Department of Physics, Indiana University, Bloomington IN, United States of America

[61] Institut für Astro- und Teilchenphysik, Leopold-Franzens-Universität, Innsbruck, Austria

[62] University of Iowa, Iowa City IA, United States of America

[63] Department of Physics and Astronomy, Iowa State University, Ames IA, United States of America

[64] Joint Institute for Nuclear Research, JINR Dubna, Dubna, Russia

[65] KEK, High Energy Accelerator Research Organization, Tsukuba, Japan

[66] Graduate School of Science, Kobe University, Kobe, Japan

[67] Faculty of Science, Kyoto University, Kyoto, Japan

[68] Kyoto University of Education, Kyoto, Japan

[69] Department of Physics, Kyushu University, Fukuoka, Japan

[70] Instituto de Física La Plata, Universidad Nacional de La Plata and CONICET, La Plata, Argentina

[71] Physics Department, Lancaster University, Lancaster, United Kingdom

[72] [a] INFN Sezione di Lecce; [b] Dipartimento di Matematica e Fisica, Università del Salento, Lecce, Italy

[73] Oliver Lodge Laboratory, University of Liverpool, Liverpool, United Kingdom

[74] Department of Physics, Jožef Stefan Institute and University of Ljubljana, Ljubljana, Slovenia

[75] School of Physics and Astronomy, Queen Mary University of London, London, United Kingdom

[76] Department of Physics, Royal Holloway University of London, Surrey, United Kingdom

[77] Department of Physics and Astronomy, University College London, London, United Kingdom

[78] Laboratoire de Physique Nucléaire et de Hautes Energies, UPMC and Université Paris-Diderot and CNRS/IN2P3, Paris, France

[79] Fysiska institutionen, Lunds universitet, Lund, Sweden

[80] Departamento de Fisica Teorica C-15, Universidad Autonoma de Madrid, Madrid, Spain

[81] Institut für Physik, Universität Mainz, Mainz, Germany

[82] School of Physics and Astronomy, University of Manchester, Manchester, United Kingdom

[83] CPPM, Aix-Marseille Université and CNRS/IN2P3, Marseille, France

[84] Department of Physics, University of Massachusetts, Amherst MA, United States of America

[85] Department of Physics, McGill University, Montreal QC, Canada

[86] School of Physics, University of Melbourne, Victoria, Australia

[87] Department of Physics, The University of Michigan, Ann Arbor MI, United States of America

[88] Department of Physics and Astronomy, Michigan State University, East Lansing MI, United States of America

[89] [a] INFN Sezione di Milano; [b] Dipartimento di Fisica, Università di Milano, Milano, Italy

[90] B.I. Stepanov Institute of Physics, National Academy of Sciences of Belarus, Minsk, Republic of Belarus

[91] National Scientific and Educational Centre for Particle and High Energy Physics, Minsk, Republic of Belarus

[92] Department of Physics, Massachusetts Institute of Technology, Cambridge MA, United States of America

[93] Group of Particle Physics, University of Montreal, Montreal QC, Canada

[94] P.N. Lebedev Institute of Physics, Academy of Sciences, Moscow, Russia

[95] Institute for Theoretical and Experimental Physics (ITEP), Moscow, Russia

[96] Moscow Engineering and Physics Institute (MEPhI), Moscow, Russia

[97] Skobeltsyn Institute of Nuclear Physics, Lomonosov Moscow State University, Moscow, Russia

[98] Fakultät für Physik, Ludwig-Maximilians-Universität München, München, Germany

[99] Max-Planck-Institut für Physik (Werner-Heisenberg-Institut), München, Germany

[100] Nagasaki Institute of Applied Science, Nagasaki, Japan

[101] Graduate School of Science and Kobayashi-Maskawa Institute, Nagoya University, Nagoya, Japan

[102] [a] INFN Sezione di Napoli; [b] Dipartimento di Scienze Fisiche, Università di Napoli, Napoli, Italy

[103] Department of Physics and Astronomy, University of New Mexico, Albuquerque NM, United States of America

[104] Institute for Mathematics, Astrophysics and Particle Physics, Radboud University Nijmegen/Nikhef, Nijmegen, Netherlands

[105] Nikhef National Institute for Subatomic Physics and University of Amsterdam, Amsterdam, Netherlands

[106] Department of Physics, Northern Illinois University, DeKalb IL, United States of America

[107] Budker Institute of Nuclear Physics, SB RAS, Novosibirsk, Russia

[108] Department of Physics, New York University, New York NY, United States of America

[109] Ohio State University, Columbus OH, United States of America

[110] Faculty of Science, Okayama University, Okayama, Japan

[111] Homer L. Dodge Department of Physics and Astronomy, University of Oklahoma, Norman OK, United States of America

[112] Department of Physics, Oklahoma State University, Stillwater OK, United States of America

[113] Palacký University, RCPTM, Olomouc, Czech Republic

[114] Center for High Energy Physics, University of Oregon, Eugene OR, United States of America

[115] LAL, Université Paris-Sud and CNRS/IN2P3, Orsay, France

[116] Graduate School of Science, Osaka University, Osaka, Japan

[117] Department of Physics, University of Oslo, Oslo, Norway

[118] Department of Physics, Oxford University, Oxford, United Kingdom

[119] [a] INFN Sezione di Pavia; [b] Dipartimento di Fisica, Università di Pavia, Pavia, Italy

[120] Department of Physics, University of Pennsylvania, Philadelphia PA, United States of America

[121] Petersburg Nuclear Physics Institute, Gatchina, Russia

[122] [a] INFN Sezione di Pisa; [b] Dipartimento di Fisica E. Fermi, Università di Pisa, Pisa, Italy

[123] Department of Physics and Astronomy, University of Pittsburgh, Pittsburgh PA, United States of America

[124] [a] Laboratorio de Instrumentacao e Fisica Experimental de Particulas - LIP, Lisboa, Portugal; [b] Departamento de Fisica Teorica y del Cosmos and CAFPE, Universidad de Granada, Granada, Spain

[125] Institute of Physics, Academy of Sciences of the Czech Republic, Praha, Czech Republic

[126] Faculty of Mathematics and Physics, Charles University in Prague, Praha, Czech Republic

[127] Czech Technical University in Prague, Praha, Czech Republic

[128] State Research Center Institute for High Energy Physics, Protvino, Russia

[129] Particle Physics Department, Rutherford Appleton Laboratory, Didcot, United Kingdom

[130] Physics Department, University of Regina, Regina SK, Canada

[131] Ritsumeikan University, Kusatsu, Shiga, Japan

[132] [a] INFN Sezione di Roma I; [b] Dipartimento di Fisica, Università La Sapienza, Roma, Italy

[133] [a] INFN Sezione di Roma Tor Vergata; [b] Dipartimento di Fisica, Università di Roma Tor Vergata, Roma, Italy

[134] [a] INFN Sezione di Roma Tre; [b] Dipartimento di Fisica, Università Roma Tre, Roma, Italy

[135] [a] Faculté des Sciences Ain Chock, Réseau Universitaire de Physique des Hautes Energies - Université Hassan II, Casablanca; [b] Centre National de l'Energie des Sciences Techniques Nucleaires, Rabat; [c] Faculté des Sciences Semlalia, Université Cadi Ayyad, LPHEA-Marrakech; [d] Faculté des Sciences, Université Mohamed Premier and LPTPM, Oujda; [e] Faculté des sciences, Université Mohammed V-Agdal, Rabat, Morocco

[136] DSM/IRFU (Institut de Recherches sur les Lois Fondamentales de l'Univers), CEA Saclay (Commissariat a l'Energie Atomique), Gif-sur-Yvette, France

[137] Santa Cruz Institute for Particle Physics, University of California Santa Cruz, Santa Cruz CA, United States of America

[138] Department of Physics, University of Washington, Seattle WA, United States of America

[139] Department of Physics and Astronomy, University of Sheffield, Sheffield, United Kingdom

[140] Department of Physics, Shinshu University, Nagano, Japan

[141] Fachbereich Physik, Universität Siegen, Siegen, Germany

[142] Department of Physics, Simon Fraser University, Burnaby BC, Canada

[143] SLAC National Accelerator Laboratory, Stanford CA, United States of America

[144] [a] Faculty of Mathematics, Physics & Informatics, Comenius University, Bratislava; [b] Department of Subnuclear Physics, Institute of Experimental Physics of the Slovak Academy of Sciences, Kosice, Slovak Republic

[145] [a] Department of Physics, University of Johannesburg, Johannesburg; [b] School of Physics, University of the Witwatersrand, Johannesburg, South Africa

[146] [a] Department of Physics, Stockholm University; [b] The Oskar Klein Centre, Stockholm, Sweden

[147] Physics Department, Royal Institute of Technology, Stockholm, Sweden

[148] Departments of Physics & Astronomy and Chemistry, Stony Brook University, Stony Brook NY, United States of America

[149] Department of Physics and Astronomy, University of Sussex, Brighton, United Kingdom

[150] School of Physics, University of Sydney, Sydney, Australia

[151] Institute of Physics, Academia Sinica, Taipei, Taiwan

[152] Department of Physics, Technion: Israel Institute of Technology, Haifa, Israel

[153] Raymond and Beverly Sackler School of Physics and Astronomy, Tel Aviv University, Tel Aviv, Israel

[154] Department of Physics, Aristotle University of Thessaloniki, Thessaloniki, Greece

[155] International Center for Elementary Particle Physics and Department of Physics, The University of Tokyo, Tokyo, Japan

[156] Graduate School of Science and Technology, Tokyo Metropolitan University, Tokyo, Japan

[157] Department of Physics, Tokyo Institute of Technology, Tokyo, Japan

[158] Department of Physics, University of Toronto, Toronto ON, Canada

[159] [a] TRIUMF, Vancouver BC; [b] Department of Physics and Astronomy, York University, Toronto ON, Canada

[160] Faculty of Pure and Applied Sciences, University of Tsukuba, Tsukuba, Japan

[161] Department of Physics and Astronomy, Tufts University, Medford MA, United States of America

[162] Centro de Investigaciones, Universidad Antonio Narino, Bogota, Colombia

[163] Department of Physics and Astronomy, University of California Irvine, Irvine CA, United States of America

[164] (a) INFN Gruppo Collegato di Udine; (b) ICTP, Trieste; (c) Dipartimento di Chimica, Fisica e Ambiente, Università di Udine, Udine, Italy

[165] Department of Physics, University of Illinois, Urbana IL, United States of America

[166] Department of Physics and Astronomy, University of Uppsala, Uppsala, Sweden

[167] Instituto de Física Corpuscular (IFIC) and Departamento de Física Atómica, Molecular y Nuclear and Departamento de Ingeniería Electrónica and Instituto de Microelectrónica de Barcelona (IMB-CNM), University of Valencia and CSIC, Valencia, Spain

[168] Department of Physics, University of British Columbia, Vancouver BC, Canada

[169] Department of Physics and Astronomy, University of Victoria, Victoria BC, Canada

[170] Department of Physics, University of Warwick, Coventry, United Kingdom

[171] Waseda University, Tokyo, Japan

[172] Department of Particle Physics, The Weizmann Institute of Science, Rehovot, Israel

[173] Department of Physics, University of Wisconsin, Madison WI, United States of America

[174] Fakultät für Physik und Astronomie, Julius-Maximilians-Universität, Würzburg, Germany

[175] Fachbereich C Physik, Bergische Universität Wuppertal, Wuppertal, Germany

[176] Department of Physics, Yale University, New Haven CT, United States of America

[177] Yerevan Physics Institute, Yerevan, Armenia

[178] Centre de Calcul de l'Institut National de Physique Nucléaire et de Physique des Particules (IN2P3), Villeurbanne, France

[a] Also at Laboratorio de Instrumentacao e Fisica Experimental de Particulas - LIP, Lisboa, Portugal

[b] Also at Faculdade de Ciencias and CFNUL, Universidade de Lisboa, Lisboa, Portugal

[c] Also at Particle Physics Department, Rutherford Appleton Laboratory, Didcot, United Kingdom

[d] Also at TRIUMF, Vancouver BC, Canada

[e] Also at Department of Physics, California State University, Fresno CA, United States of America

[f] Also at Novosibirsk State University, Novosibirsk, Russia

[g] Also at Fermilab, Batavia IL, United States of America

[h] Also at Department of Physics, University of Coimbra, Coimbra, Portugal

[i] Also at Department of Physics, UASLP, San Luis Potosi, Mexico

[j] Also at Università di Napoli Parthenope, Napoli, Italy

[k] Also at Institute of Particle Physics (IPP), Canada

[l] Also at Department of Physics, Middle East Technical University, Ankara, Turkey

[m] Also at Louisiana Tech University, Ruston LA, United States of America

[n] Also at Dep Fisica and CEFITEC of Faculdade de Ciencias e Tecnologia, Universidade Nova de Lisboa, Caparica, Portugal

[o] Also at Department of Physics and Astronomy, University College London, London, United Kingdom

[p] Also at Group of Particle Physics, University of Montreal, Montreal QC, Canada

[q] Also at Department of Physics, University of Cape Town, Cape Town, South Africa

[r] Also at Institute of Physics, Azerbaijan Academy of Sciences, Baku, Azerbaijan

[s] Also at Institut für Experimentalphysik, Universität Hamburg, Hamburg, Germany

[t] Also at Manhattan College, New York NY, United States of America

[u] Also at School of Physics, Shandong University, Shandong, China

[v] Also at CPPM, Aix-Marseille Université and CNRS/IN2P3, Marseille, France

[w] Also at School of Physics and Engineering, Sun Yat-sen University, Guanzhou, China

[x] Also at Academia Sinica Grid Computing, Institute of Physics, Academia Sinica, Taipei, Taiwan

[y] Also at Dipartimento di Fisica, Università La Sapienza, Roma, Italy

[z] Also at DSM/IRFU (Institut de Recherches sur les Lois Fondamentales de l'Univers), CEA Saclay (Commissariat a l'Energie Atomique), Gif-sur-Yvette, France

[aa] Also at Section de Physique, Université de Genève, Geneva, Switzerland

[ab] Also at Departamento de Fisica, Universidade de Minho, Braga, Portugal

[ac] Also at Department of Physics and Astronomy, University of South Carolina, Columbia SC, United States of America

[ad] Also at Institute for Particle and Nuclear Physics, Wigner Research Centre for Physics, Budapest, Hungary

[ae] Also at California Institute of Technology, Pasadena CA, United States of America

[af] Also at Institute of Physics, Jagiellonian University, Krakow, Poland

[ag] Also at LAL, Université Paris-Sud and CNRS/IN2P3, Orsay, France

[ah] Also at Nevis Laboratory, Columbia University, Irvington NY, United States of America

[ai] Also at Department of Physics and Astronomy, University of Sheffield, Sheffield, United Kingdom

[aj] Also at Department of Physics, Oxford University, Oxford, United Kingdom

[ak] Also at Institute of Physics, Academia Sinica, Taipei, Taiwan

[al] Also at Department of Physics, The University of Michigan, Ann Arbor MI, United States of America

[am] Also at Discipline of Physics, University of KwaZulu-Natal, Durban, South Africa

* Deceased